Mass Loss, Destruction and Detection of Sun-grazing & -impacting Cometary Nuclei

J.C. Brown[1], H.E. Potts[1], L.J. Porter[1,2] & G. le Chat[1,3]

[1] School of Physics & Astronomy, University of Glasgow, G12 8QQ, UK. e-mail: `john@astro.gla.ac.uk`

[2] Max-Planck-Institut für Astrophysik, D-85748 Garching, Germany

[3] LESIA, Observatoire de Paris, CNRS, UPMC, Université Paris Diderot; 92190 Meudon, France

July 7, 2011

ABSTRACT

Context. Incoming sun-grazing comets almost never re-emerge, but no final destruction event has ever been observed, nor sun-impactor destruction theory developed. NOTE ADDED 7/7/11- Shortly after this paper was resubmitted (21/6/11) to A&A, actual observations of destruction of a sun-grazer comet today were reported by Shryver - see www.lmsal.com/ schryver/

Aims. We seek analytic models of comet nucleus destruction at the sun, to estimate impact signature dependence on incident mass Mo and perihelion q.

Methods. We approximate evaporative mass loss rates by heating rate/latent heat of sublimation and obtain analytic estimates for M(r) versus q and distance r for evaporation processes alone - insolation sublimation and, for the first time, impact ablation. Insolation dominates above 1.01Rsun (density n below 2.5E11/cc). Below 1.01Rsun, ablation overwhelms insolation, since n(r) rises exponentially. Nuclei with Mo(1-q/1.01Rsun)**1.5 below 1E10 g are totally ablated before ram pressure matters. This shallow entry angle regime applies to the great majority of sun-grazers but any high mass/steep entry nuclei penetrate to n above 2.5E14/cc where soaring ram pressure drives catastrophic explosion like large mass comet-planet impacts.

Results. Close sun-grazers fall sharply into three (Mo,q) regimes: insolation-, ablation-, and explosion-dominated. Our analytic insolation regime results are similar to previous numerical models. Nuclei of Mo exceeding 1E11 g either survive insolation to r=1.01Rsun and re-emerge or, for q below 1.01Rsun, enter the atmospheric collisional regime where behavior depends on Mo and entry angle phi. For the shallow angle impacts of most sun-grazers, all but the heaviest nuclei ablate totally before exploding, though the hot wake itself explodes. For steep entry, all masses explode before total ablation, creating an airburst and fireball. These explosions resemble solar flares and should be observable.

Conclusions. Analytic descriptions indicate the (Mo,q) regimes where sublimation, ablation and explosion dominate destruction of sun-grazer/-impactor comets. Extended insolative destruction near the sun is hard to observe. Nuclei with q below 1.01Rsun and Mo above 1E11 g are destroyed catastrophically by ablation or explosion (depending on Mo(cos phi)**3) in the chromosphere, producing fireballs with properties comparable to solar flares but with cometary abundance spectra. Only nuclei more massive than 1E17 g can ever reach the photosphere before exploding.

Key words. comet; sun; impact; sun-grazing; radiation; collisions

[1]

1. Introduction

'Sun-grazing' comets were once thought to be very rare but are now discovered almost daily. Many of these have perihelion distances q close to, and some less than, a solar radius $R_\odot$ (see e.g. Sekanina 2002, 2003, Marsden 2005 and http://www.minorplanetcenter.org/mpec/RecentMPECs.html). Early use of the term 'sun-grazers' referred to any $q \leq 10R_\odot$ but the recent numerous discoveries mainly have $q \approx R_\odot$. Only a very few of these close sun-grazers, discovered as they near the sun, has ever been seen to re-emerge (Marsden 2005),

presumably because most are vaporized and dispersed in the sun's close proximity, though these final death throes have never been seen directly (but cf. Sekanina 1982). Such facts alone can set upper limits to the masses of nuclei, as we discuss later. Some have $q < 1$ (Sekanina 2002, Marsden 2005) but the closest alleged direct observation of a comet was the HAO patrol H-α image proposed by Raftery et al. (2010) to be Comet C/2010 E6 (STEREO) approaching perihelion $q = (1.020 \pm 0.005)R_\odot$. In a very detailed search Brown, McIntosh and Battams (2011 in preparation) did not find the location, timing, or motion of this H-α feature to match that of C/2010 E6, nor did they find any notable matching feature in SoHO or STEREO data, the latter covering the back side of the sun where perihelion occurred. Raftery et al. have now withdrawn their H-α claim for similar reasons (P. St Hilaire 2011 personal communication). Thus the search goes on for direct observations of the terminal deaths of sun-grazing comets and the exciting opportunity to measure abundances from them despite the fact, as we prove below, that cometary nuclei of $q < 1.01R_\odot$, $M_o > 10^{11}$ g undergo catastrophic destruction by interaction with the dense lower

---

solar atmosphere, releasing energies and involving plasma masses comparable to those of solar flares though of very different scales and chemical abundances. Direct observation of these sun impacting comet explosions, or of the more gradual destruction by insolation in the corona of sun-grazing or low mass comets, should be of great interest to solar and cometary physicists. Modeling of the destruction processes and their radiation signatures is an essential step in searching for them and in interpreting them once seen. Interest in cometary impacts has been further enhanced recently by the three further impacts on Jupiter in the last year or so while the Shoemaker-Levy 9 Jupiter impacts of mid-July 1994 greatly stimulated modeling of comet-atmospheric impacts (e.g. Carlson et al. 1997), as we discuss below.

The processes leading to sublimation of the icy conglomerate mix (Whipple 1950) of cometary nuclei, and in some cases their splitting and fragmentation, as they approach the sun, have been considered by Huebner (1967), Weissman and Kieffer (1982), Weissman (1983), Iseli et al. (2002), Sekanina (2003) and others. In essence all of these models solve for the sublimation mass loss rates of icy-conglomerate mixes driven by absorption of sunlight (the dust being carried away in the flow of these gasified components). These models allow, to varying degrees, for the complicating factors of rotation, albedo, insulating surface dust layers, radiative cooling, and thermal conduction into the interior, and sometimes fragmentation by tidal, thermal and volatile explosion effects. However, Huebner (1967) and Iseli et al. (2002), for example, found that, for high sublimation rates near the sun, many of these effects were secondary, the mass loss rate being reasonably approximated by a pure sublimation description : mass loss rate = heating rate/effective latent heat of sublimation. Sekanina (2003) addressed in detail how mass loss rates relate to cometary light curves via emission (e.g. by sodium) and by dust scattering of sunlight, tying his modeling to data from SoHO. He emphasized the importance of fragmentation in considering light curves but noted that most of the mass remains in a primary 'fragment'. In all of these studies the sole heating process considered was insolation. None considered either direct ablation or ram-pressure driven explosion due to solar atmospheric impact (which are in fact negligible till $r \lesssim 1.01 R_\odot$ as we show below) though, in his discussion of insolation sublimation, Weissman (1983) remarked *"ultimate destruction of the nucleus [of sun-impacting comets] likely results from the shock of hitting the denser regions of the solar atmosphere"*. It is well known in the planetary physics community that explosion, and ablation, are key elements in the destruction of comets impacting planetary atmospheres (e.g. Carslon et al. 1993).

In this paper we revisit the treatment of icy conglomerate nucleus mass loss rates on approach to the sun due purely to insolation sublimation but then develop, for the first time, estimates of the much higher ablation mass loss rates in very close approaches due to solar atmospheric bombardment (which we term 'atmospheric ablation'). We show that for $q \lesssim 1.01 R_\odot$ the exponential increase in atmospheric density with depth results in atmospheric ablation (and ram pressure for higher masses) totally overwhelming insolation sublimation in the upper chromosphere. As discussed further in Sections 3.4, 6.1, 6.2, this regime is similar to that of comets impacting planetary atmospheres though with the following important differences

– The impact speed $v_\odot$ is much higher ($\sim 10\times$) than that of planetary impacts. Consequently the energy deposition needed for total ablation is an even smaller fraction $\sim 10^{-5}$ of the total kinetic energy than for e.g. Jupiter ($\sim 10^{-3}$).

– The solar chromospheric temperature, hydrogen ionization, and density scale height are all much larger than Jupiter's, and the density n much lower at a given column mass

– Almost all known sun-grazing 'comets' are members of secondary comet 'groups' like the Kreutz Group (e.g. Marsden 2005) and have small mass and very shallow incidence angles (since $q \approx R_\odot$). As we show, combined with the above points, this has major implications for the relative importance of ablation and explosion compared with the case of planetary impacts.

This bombardment results in extremely rapid loss (by ablation and explosion) of nucleus mass, momentum and kinetic energy. The soaring temperature and pressure lead to destructive detonation of the nucleus and its wake. This 'air burst' is followed by explosive expansion of the resulting 'fireball' of cometary and solar atmospheric material. The total masses and energies of these explosive sun-impacting events are in roughly the same range as those of solar magnetic flares, though the size and time scales of the initial detonation are much smaller, and the nucleus/airburst density much higher, than those in magnetic flares. We coin the term 'cometary flare' to describe such explosive comet destruction by atmospheric collisions near the sun's surface. A significant number of comets must have $q < R_\odot$ (Hughes 2001) and large enough mass ($M_o \gtrsim 10^{11}$ g - see Section 5, Equation (28)) to survive insolation down to the intense atmospheric ablation/explosion regime. Comet C/2010 E6 (STEREO) discussed by Raftery et al. (2010) had $q \approx 1.02 R_\odot$ which means that it narrowly missed causing a cometary flare by ablative destruction (if its mass were large enough to survive sublimation by insolation).

We first (Section 2) discuss the order of magnitude of relevant nucleus parameters then (Section 3) estimate roughly the relative importance and time/distance scales of nucleus mass loss (insolation and ablation), explosion and deceleration processes. We conclude that, for small masses ($\lesssim 10^{11}$ g) and/or $q \gtrsim 1.01 R_\odot$) only insolation mass loss matters and that it occurs as a relatively gentle 'fizzle' over a distance scale of order $R_\odot$ (timescale ≈ 1000 s). For comets with $q < 1.01 R_\odot$ and massive enough to penetrate beyond that point, insolation is negligible there compared with atmospheric impacts. We consider the latter by drawing on the planetary impact literature, modified to solar and sun-grazer parameters, the results depending on incident mass and, critically, on incidence angle (i.e. on $q/R_\odot$). We find that for small masses, or quite large masses with the shallow incidence typical of sun-grazers/impactors, nucleus ablation is complete before the nucleus itself explodes (unlike the case of the steep Jupiter impacts of Shoemaker-Levy 9), though the vaporized wake material loses its kinetic energy very abruptly and itself explodes. For all but very small masses, steep entry angles result in ram pressure-driven explosive expansion of the nucleus which surpasses the pure ablation rate and enhances both it and deceleration. Explosion is thus the key element in final destruction of such nuclei. In all cases the resulting chromospheric 'airburst' subsequently evolves as a 'fireball' exploding upward in the overlying solar atmosphere (cf. Carlson et al 1997).

Following these rough estimates and conclusions, we first consider in some detail an approximate analytic treatment of the simplest, and most relevant, cases of mass loss purely by insolation sublimation and purely by atmospheric ablation . For the case of sun-impactors (Sections 3.4.2 and 6.1), total ablation occurs over about a chromospheric scale height $H \approx 500$km (timescale ≈ 1 s) the kinetic energy and momentum of the ablated matter being then converted into intense heating and ex-

plosive expansion of the cometary and surrounding atmospheric plasmas. We then consider more briefly the rarer steep impact cases and. drawing on the planetary impact literature, estimate the properties of the resulting pressure driven catastrophic explosion of the nucleus itself. Over a very large range of masses and impact angles the final destruction of the nucleus by ablation/explosion occurs over a height range of only a few scale heights in the chromosphere, depending only logarithmically on the mass.

2. Comet Nucleus Parameters and Perihelia

2.1. Preamble

As mentioned above and discussed in more detail below, cometary nuclei undergo mass loss by absorption of energy in the form of insolation and atmospheric bombardment. These cause sublimation and ablation of mass from the energy absorbing surface but also deliver heat and shock waves into the interior of the nucleus and of the mass loss wake which can result in their explosive destruction. The relative importance of the various processes involved depends on the properties of the nucleus and of the incident energy flux. We first (Section 2.2) discuss these properties before assessing (Section 3) the relative importance of sublimation, ablation, explosion and deceleration processes in comet destruction. In Section 2.3 we briefly discuss the issue of comet perihelion frequency distribution $N_q(q)$ emphasizing the difference between that for primary comets which have $N_q(q)$ quite uniform in q (Hughes 2000) and that for the much more numerous Group (e.g. Kreutz) comets from a single progenitor which are concentrated near $q = R_\odot$.

2.2. Properties of Nucleus material

2.2.1. Masses and Densities

Over the years, there has been a wide variation of opinion over the masses M_o and mean mass densities ρ of the icy-conglomerate mix which cometary nuclei are thought to comprise - Whipple (1950), over how well we know these for any specific comet, and over how widely the values vary between comets. We will take the incident mass M_o to be a parameter and present results for the mass range $M_o \approx 10^9 - 10^{20}$ g which should span from the faintest comets detected almost daily by SoHO etc to the largest super-massive comets (of order $10^2 - 10^4$ times typical mass estimates for Halley and for Hale Bopp). At solar escape speed $v_\odot = 618$ km/s (perihelion speed for $q = R_\odot$), this mass range corresponds to kinetic energies of about $10^{24} - 10^{36}$ erg. For comparison we note that the plasma masses heated in and ejected by solar magnetic flares are in the range $\sim 10^9 - 10^{16}$ g from nanoflares to giant flares with magnetic energy released $\sim 10^{26} - 10^{33}$ erg.

Concerning the density ρ, MacLow and Zhanle 1994 said *"the density of comets is the stuff of speculation [probably] 0.3 - 1.0 g/cm³ but with extreme claims of 0.01-5"* while in his insolation sublimation modeling Sekanina (2003) used $\rho = 0.15$ g/cm³. More recently, however, Weissman and Lowry (2008) critically discussed results from a range of methods, including Deep Impact data, all with a considerable error range, but conclude that $\rho = 0.6 \pm 0.2$ g/cm³ is the most likely range for the comets they studied. A considerable spread in ρ between comets seems likely, especially if one includes very large comets (which are rare) and very small ones (which are hard to measure). Here we will simply take ρ as a parameter of the problem, and express

it relative to that of (water) ice $\rho_{ice} = 0.9$ g/cm³ via a dimensionless scaling parameter

$$\tilde{\rho} = \rho/\rho_{ice} \tag{1}$$

In discussing results we mainly use a mean value $\tilde{\rho} = 0.5$ ($\rho \approx 0.45$ g/cm³) though showing how results, such as for M_o, can be scaled for other values (see Equation (21) and Figure 1).

2.2.2. Physical Strength and Sound Speed

The effects on the nucleus of the pressure associated with the energy fluxes driving sublimation/ablation depend on how strong the nucleus material is and how fast pressure waves propagate through its volume. In the initial stages the relevant strength is that of the ice-conglomerate mix, estimated by Zhanle and MacLow (1994) to be a pressure ($\approx$ energy density) of $P_c \approx 10^6$ dyne/cm²($\equiv$ erg/cm³). Values discussed, however, range from 10^5 for very fluffy snowy structures to 10^8 for very solid asteroid-like bodies (Chyba et al 1993). Here we will use $P_c = 10^6$ dyne/cm² but it should be borne in mind that the quantitative regimes of relative importance of ablation and hydrodynamic explosion depend on its value. For the sound speed, Zhanle and MacLow (1994) suggest $c_s \approx 1 - 3 \times 10^5$ cm/s for the initial state nucleus material. Values for a range of more or less solid material do not differ greatly.

2.2.3. Latent heat of sublimation

The major cometary nucleus parameter determining its rate of mass loss for power input $\mathcal{P}$ erg/s is the latent heat $\mathcal{L}$ (erg/g) of sublimation/ablation for the cometary ice-conglomerate mix. The value for water ice is about 2.6×10^{10} erg/g and is of order the relevant value when the mass lost is in the form of water vapor whose pressure sweeps dust and other non-volatiles away with it. However, in situations of intense heating, such as atmospheric bombardment, where all components are eventually vaporized, the relevant value is the density weighted mean over all mass components, including volatile and refractory ones. Sekanina (2003) finds values for what he terms 'effective latent heat of erosion'to be around 0.3 of the water ice value. (Note that Sekanina qives values for erg/mole which differ much more widely than $\mathcal{L}$ erg/g). On the other hand adopting a component composition of mass like that given by Huebner et al. (2006) viz [Silicates : organics : carbonaceous: ices] = [0.26 : 0.23 : 0.086 : 0.426] we see that the refractory silicates are the most important non-ice component. Mendis (1975) give $\mathcal{L} = 2.30 \times 10^{10}$ erg/g for silicates, which is close to that of water ice, while the organics will tend to lower the mean slightly. Chyba et al (1993) adopted 2.3×10^{10} for comets, 5×10^{10} for carbonaceous and 8×10^{10} for stone/iron bodies and just 10^{11} even for solid iron. So we will use the water ice value for $\mathcal{L}$ as a reasonable first approximation, but include a dimensionless scaling parameter

$$\tilde{\mathcal{L}} = \mathcal{L}/\mathcal{L}_{ice} \tag{2}$$

to allow application of our expressions for other values of $\mathcal{L}$ though we will use $\tilde{\mathcal{L}} \approx 1, (\mathcal{L} \approx \mathcal{L}_{ice})$, in most numerical evaluations but show how to convert for other values - Figure 1 and Equation (21).

2.2.4. Nucleus shape and 'size'

We know from direct imaging, and from light curve data etc., that cometary nuclei are of diverse, irregular and distinctly as-

pherical shapes - e.g. rough peanut-shell like. So, for our approximate modeling purposes, we characterize them rather crudely by a single mean dimension a such that their mass $M \approx \rho a^3$ (for uniform ρ) and their direction-averaged cross-sectional area $A \approx a^2$. To get an idea of the uncertainty involved, if the shape were actually spherical with a the diameter, in our approximations of the mass by $M = \rho a^3$ and the cross section by $A = a^2$, M and A would be off by factors of $6/\pi$ and A by $4/\pi$ respectively, within the uncertainties of the shape and of the more general physics of the problem.

2.3. Perihelion Distribution of Group versus Progenitor Comets

It is important to note that the vast majority of comets seen near the sun. which we are modeling here, are not primordial comets but members of Groups (such as the Kreutz Group) of low mass fragments of a disrupted massive progenitor. As well as low masses, such comet group members typically have very similar orbits with perihelia clustered close to $q = R_\odot$. This implies very shallow entry angles (if and) when they enter the solar chromosphere. This is in contrast to the near uniform distribution of q among primordial comets (Hughes 2000) some of which (with $q \ll R_\odot$) would enter the chromosphere steeply. As we show below, low-mass/shallow entry and high-mass/steep entry comets exhibit distinctive regimes of destruction physics, the former being ablation dominated (like low mass meteors in the earth's atmosphere) and the latter explosion dominated (like steep high mass comet/asteroid-planet impacts - cf. Chyba et al. 1993 - such as Shoemaker-Levy on Jupiter - e.g. Carlson et al 1997).

3. Rough Comparison of Nucleus Mass Loss, Deceleration and Explosion Processes

3.1. 'Evaporative' Mass Loss versus Deceleration

Whether mass loss from the nucleus is by insolation sublimation or by atmospheric ablation, the total energy needed to vaporize the whole nucleus is $\mathcal{E}_{vap} = M_o \mathcal{L}$ while the energy needed to stop it is $\mathcal{E}_{kin} \approx M_o v_\odot^2/2$. The ratio is tiny, $\mathcal{E}_{vap}/\mathcal{E}_{kin} \approx 2\mathcal{L}/v_\odot^2 = 4 \times 10^{-5} \tilde{\mathcal{L}}$ for the solar escape speed

$$v = v_\odot = (2GM_\odot/R_\odot)^{1/2} \approx 618 \text{ km/s} \tag{3}$$

with $G, M_\odot, R_\odot$ the gravitational constant, solar mass, and solar radius respectively. Thus total vaporization occurs well before the nucleus decelerates significantly, even if the nucleus is undergoing explosive expansion (since this increases the area heated as well as the deceleration) - see Section 6.2. One can equivalently argue from momentum conservation that, in order to slow down, the nucleus must encounter an atmospheric mass comparable to M_o and that in doing so it absorbs an energy far greater than needed to vaporize it. The mass per unit area (g cm^{-2}) of a comet nucleus is $\Sigma_c \approx M_o/a^2 = M_o^{1/3} \rho^{2/3} = 10^4 (M_o/10^{12})^{1/3} (\tilde{\rho})^{2/3}$ g cm^{-2} while that of the sun's atmosphere even down to the photosphere is only $\Sigma_\odot \approx 1$ g cm^{-2}. Consequently, unless they explode, increasing the deceleration, only objects of $< 10^3$ g or so would be much decelerated by the mass of the sun's atmosphere down to the photosphere (though, in practice, they would be vaporized by insolation and/or ablation long before reaching it). Note also that, at infall speed $v_\odot$, in the frame of the nucleus solar atmospheric protons have kinetic energy, ~ 2 keV which is enough to ablate 10 water ice molecules). This situation of initial ablative mass without significant deceleration is paralleled by the dynamics in planetary atmospheres of meteors - e.g. McKinley (1961), Kaiser (1962) - and at least of the initial (high altitude) stages of comet-planet impacts - cf. Shoemaker Levy 9 with Jupiter - cf. Section 6.2.

For insolation sublimation there is the further specific point that for light the ratio of energy to momentum flux is (because of the high speed of light $c = 3 \times 10^{10}$ cm/s) very high compared to that for matter. Consequently the radiation pressure force F_{rad} has negligible effect on the nucleus speed though it delivers a large amount of energy. Specifically the ratio of F_{rad} to the gravitational force is (ignoring the correction factor 1.0-2.0 for albedo)

$$\frac{F_{rad}}{F_{grav}} = \frac{L_\odot a^2}{4\pi GM_\odot c \rho a^3} = \frac{10^{-4}}{a(cm)\tilde{\rho}} \tag{4}$$

Thus $\frac{F_{rad}}{F_{grav}} \ll 1$ for all solid objects much larger than a micron. The radiation pressure $F_{rad}/c \simeq 2$ erg/cm^3 is also tiny compared to the nucleus strength P_c so insolation causes no direct explosion effects.

In Appendix A, we show further that the rocket effect of mass loss leaving the nucleus anisotropically also has negligible effect on v during vaporisation, essentially because the very high nucleus ρ value implies very low mass loss speed u and hence momentum flux. Consequently, the velocity of the nucleus during its vaporisation is well approximated by that of a gravitational parabolic orbit, viz., in orbital plane polar coordinate (r, θ) and for perihelion distance q

$$v_\theta = r\dot{\theta} = v_\odot \left(\frac{R_\odot}{r}\right)^{1/2} \left(\frac{q}{r}\right)^{1/2}$$

$$v_r = \dot{r} = v_\odot \left(\frac{R_\odot}{r}\right)^{1/2} \left(1 - \frac{q}{r}\right)^{1/2}$$

$$v = (v_\theta^2 + v_r^2)^{1/2} = v_\odot \left(\frac{R_\odot}{r}\right)^{1/2} \tag{5}$$

3.2. Deceleration of sublimated/ablated mass

While, throughout the total vaporization lifetime of the nucleus, its velocity is well described by Equations (5), this is not true at all of the material lost from the nucleus since, once small particles leave the nucleus they will not obey Equations (5), non-gravitational accelerations on them being much larger. In particular, the radiation pressure force on any small solid particles (less than a micron) is higher than gravity, as they have much higher surface to mass ratio ($\propto 1/a$) than the comet nucleus. More importantly, small particles, atoms and ions sublimated or ablated from the nucleus experience very high collisional drag even in the corona and are stopped abruptly. From Emslie (1978), the Coulomb collisional stopping column density for a proton of speed $v_\odot \approx 618$ km sec^{-1} (~ 2 keV) in a plasma of mainly ionized hydrogen is around $\mathcal{N}_s = 10^{15}$ cm^{-2}. Thus the stopping distance at number density n is $d \approx \mathcal{N}/n \approx 10^{15}/n$ and even less for ions of higher charge. d is thus just 1 km in the corona ($n \approx 10^{10}$ cm^{-3}) and only 0.1 mm at the photosphere ($n \approx 10^{17}$ cm^{-3}) - both tiny compared to the distances over which the nucleus itself slows. Consequently, once ablated dust particles and ions leave the nucleus and enter the solar atmosphere they stop abruptly and form a hot exploding wake as they blend with and heat the atmosphere/wind creating large local enhancements of heavy element abundance potentially detectable spectroscopically or directly in space (cf. Iseli et al 2002).

3.3. Insolation sublimation case $q \geq r_*, M_o \leq 10^{11}$ g

From the above we know that the radiation pressure force is very small compared to gravity and to the strength of nucleus material so, apart possibly from tidal force fragmentation, the dominant process in the insolation case is mass loss by sublimation with no hydrodynamic explosion (in contrast to the atmospheric collisional ablation case). Near the sun, the timescale for sublimation of the whole mass is $\tau_{sub} \geq M_o \mathcal{L}/a_o^2 \mathcal{F}_\odot \approx 4 \times 10^3 M_{12}^{1/3} \tilde{\rho}^{2/3} \tilde{\mathcal{L}}$ s, where $\mathcal{F}_\odot = 6 \times 10^{10}$ erg/cm^2/s is the bolometric photospheric flux and $M_{12} = M_o/10^{12}$ g. The corresponding distance scale is roughly $d_{sub} \approx v_\odot \tau_{sub} \approx 3.5 R_\odot \times M_{12}^{1/3} \tilde{\rho}^{2/3} \tilde{\mathcal{L}}$. The mass loss process is therefore rather gradual and extended in space so may be challenging to observe directly amid the generally dynamic state of the solar amosphere, though the anomalous (non-solar) chemical abundances in spectral data should help. As discussed more accurately in the analytic sublimation solution below (Section 5) we can also already conclude that total sublimation occurs in a close perihelion passage roughly for $d_{sub} \leq R_\odot$ which is the case for masses $M_o \leq 3 \times 10^{10}/\tilde{\rho}^2 \tilde{\mathcal{L}}^3$ g or about 10^{11}g for $\tilde{\rho} = 0.5, \tilde{\mathcal{L}} = 1$. This gives an indication of an upper limit to the masses of the great majority of sun-grazers (eg SOHO/STEREO Kreutz group) which do not reach the chromospheric ablation regime ($r \leq 1.01 R_\odot$) but are never seen to re-emerge. This diagnostic is discussed more fully and accurately in Section 5.2.3.

3.4. Atmospheric ablation and ram pressure explosion case

3.4.1. Background

The problems of comet, asteroid, and even large meteoroid impact with planetary atmospheres closely parallel those of a solar impact, though the parameter regimes are rather different, and there is no planetary equivalent of insolation. Unlike the solar case, planetary impacts have been addressed in detail, early work including that of Revelle (1979) and others, but progress was greatly accelerated in anticipation, and in the aftermath, of the collisions of fragments of Comet Shoemaker-Levy 9 with Jupiter in July 1994. Many authors (e.g. Ahrens et al. 1993, Chyba et al 1993, Sekanina 1993, Chevalier and Sarazin 1994, Zahnle and MacLow 1994) developed semi-analytic and numerical models to predict what should be expected of these impacts. Others, notably MacLow and Zahnle (1994), Field and Ferrara (1995) and Carlson et al. (1995, 1997), developed models further by drawing on actual event data. In particular, Carlson et al. (1995, 1997), in developing their 'heuristic model', combined data analysis, numerical simulations, and observational inputs. They identified and addressed both the 'bolide initial phase' (which we have called the detonation or airburst) and the subsequent 'fireball' exploding out from the nucleus and its wake, synthesising detailed observations of the G-fragment impact with their numerical modelling of the fireball (e.g. their Figure 7), partly based on the analytic self-similar point/line explosion theory of Sedov (1959). Based on arguments developed from Chyba et al. (1993), Zahnle and MacLow (1994) and MacLow and Zahnle (1994) show that the airburst phase is dominated by ablation only in the upper atmosphere, and below that by pressure-driven catastrophic disruption. In the Jupiter case, the latter is true for all impacting masses except those very much smaller than that ($\approx 10^{15}$ g) of the Shoemaker-Levy 9 fragments in 1994. However, both the initial ablation and disruptive pressure timescales are shorter than that for deceleration loss of nucleus kinetic energy, which is what ultimately powers the final explosion of the nucleus and its wake. We summarize here the essence of the arguments leading to these conclusions so that we can adapt them to the rather different conditions of solar impacts.

3.4.2. Rough comparison of the importance of impact processes

The relative importance of ablation, explosion and deceleration in the initial destruction of the nucleus depends on atmospheric scale height H as well as on the nucleus mass, speed and entry angle. They can be expressed in terms of the local atmospheric proton space density n cm^{-3} and the column density $\mathcal{N}(\text{cm}^{-2}) = \int_s n ds$ traversed *along the path of the nucleus* (as opposed to N vertically with $N = \mathcal{N} \cos \phi$ for constant angle ϕ to the vertical) after which each of the above processes would be 'complete'. First, to deliver enough energy to ablate the whole mass (without expansion) requires an encounter with column density $\mathcal{N}_{abl}$ such that $\mathcal{N}_{abl} \mu m_p v_\odot^2/2 \approx \mathcal{L} M_o/a_o^2$ where m_p is the proton mass and μ the mean mass present per H (atoms and ions) in units of m_p. This implies

$$\mathcal{N}_{abl}(\text{cm}^{-2}) = N_{abl} \sec \phi \approx \mathcal{L} M_o^{1/3} \rho^{2/3}/(\mu m_p v_\odot^2/2)$$
$$\approx 6 \times 10^{22} M_{12}^{1/3} \tilde{\mathcal{L}} \tilde{\rho}^{2/3} \quad (6)$$

On the other hand, total deceleration of the nucleus (without expansion) requires column density $\mathcal{N}_{dec}$ such that $\mathcal{N}_{dec} \mu m_p \approx M_o/a_o^2$ implying

$$\mathcal{N}_{dec}(\text{cm}^{-2}) \approx \frac{M_o^{1/3} \rho^{2/3}}{\mu m_p} \approx 4 \times 10^{27} M_{12}^{1/3} \tilde{\rho}^{2/3} \approx 3 \times 10^{27} M_{12}^{1/3} \quad (7)$$

which is $\gg \mathcal{N}_{abl}$.

For internal strength (energy density) P_c, cometary nucleus material will only undergo substantial distortion and hydrodynamic flow once it reaches the depth where atmospheric ram pressure $\mu m_p v_\odot^2/2$ approaches the value P_c. This implies a critical atmospheric proton density $n_{pres} \approx 2P_c/\mu m_p v_\odot^2$. The corresponding column density $\mathcal{N}_{pres}$ along the path depends on the atmospheric exponential scale height H and the angle ϕ according to $\mathcal{N}_{pres} = N_{pres} \sec \phi = H n_{pres} \sec \phi$ implying

$$\mathcal{N}_{pres}(\text{cm}^{-2}) = n_{pres} H \sec \phi \approx \frac{2P_c H \sec \phi}{\mu m_p v_\odot^2}$$
$$\approx 2.4 \times 10^{22} (P_c/10^6)(H/10^8) \sec \phi \quad (8)$$

Comparing Equations (6, 7) shows that, ignoring expansion of the nucleus, ablation would vaporize the whole mass long before it slowed significantly, as already argued in e.g. Section 3.1. On the other hand the ratio of the column density for ablation to that where ram pressure first significantly drives explosive expansion is given from Equations (6, 8) by

$$\frac{\mathcal{N}_{pres}}{\mathcal{N}_{abl}} \approx \frac{0.4(P_c/10^6)(H/10^8) \sec \phi}{M_{12}^{1/3} \tilde{\mathcal{L}} \tilde{\rho}^{2/3}}$$
$$\approx \frac{0.7(P_c/10^6)(H/10^8) \sec \phi}{M_{12}^{1/3}} \quad (9)$$

where the last expression is for our canonical values $\tilde{\rho} = 0.5, \tilde{\mathcal{L}} = 1$. There is thus a ($v$-independent) maximum mass $M_{abl}^{max}(\phi)$ above which destruction of the nucleus is driven by explosion rather than ablation, namely (setting ratio (9) to unity)

$$M_{abl}^{max}(\phi_*) = M_{**} \sec^3 \phi \approx 6 \times 10^{10} \left[\frac{(P_c/10^6)(H/10^8) \sec \phi}{\tilde{\mathcal{L}}\tilde{\rho}^{2/3}} \right]^3$$

$$\approx 2.4 \times 10^{11} [(P_c/10^6)(H/10^8) \sec \phi]^3 \qquad (10)$$

the last value again being for our canonical values $\tilde{\rho} = 0.5$, $\tilde{\mathcal{L}} = 1$. Note that expression (9) is v-independennt. Thus although ram pressure sets in at a lower n for the sun than for Jupiter (because v is higher) the same v dependence occurs in the ablation expression so the ratio (9) just scales as $1/H$ and reaches unity only at a higher n in the solar case. For solar values $H = 5 \times 10^7$, $P_c = 10^6$ we find $n_{pres} = n_{abl}^{end} = n_{**} = 2.5 \times 10^{14}$ cm^{-3} while $M_{**} \approx 3 \times 10^{10}$ g and $M_{abl}^{max} \approx 3 \times 10^{10} \sec^3 \phi$ g. In the case of impacts with Jupiter $H \sim 10^6 - 10^7$ (depending on height) and for relatively steep impacts ($\sec \phi \leq 2$), it is clear from Equation (9) that ram pressure will cause explosion before ablation is complete for all nuclei with masses $M_o \geq 2 \times 10^9$ g while the estimated mass of Shoemaker-Levy 9 fragments was of order 10^{15} g. Thus, as argued by Chyba et al (1993), Zahnle and MacLow (1994) and Carlson et al. (1997), for steep planetary impacts the ablation process is secondary to pressure-driven explosion except for small masses (or extremely shallow entry) and during the initial entry phase. In the case of solar chromospheric impacts, however, $H \approx 10^{7.7}$ is larger so that the maximum ablation-dominated mass (after sublimation losses) is around 3×10^{10} g for steep entry. However, for the much more usual case of sun-grazing $q \approx R_\odot$ impacts, $\sec \phi \approx 10$ for $q = R_\odot$- see Section 6.1 and $\sec \phi \gg 10$ for likely values of q for those which actually reach the ablation regime $q \leq 1.01 R_\odot$. Thus the maximum ablation-dominated mass for these is $\gg 10^{14}$ g as discussed further in Section 6.1. In Appendix B we discuss some physical factors which tend to reduce the rate of ablation below our estimate but argue that these are less important for solar than for planetary impacts.

NOTE : Throughout the rest of this paper we introduce subscripts $_*$ and $_{**}$ where $_*$ will denote quantities at the point where ablation becomes more significant than insolation, and $_{**}$ at the point where explosive expansion becomes the dominant destruction mechanism.

4. Detailed Theory of Nucleus Sublimation/Ablation

4.1. General Formulation

Having discussed orders of magnitude we now want to model the evolution of evaporative mass loss along the comet path. We take the nucleus to have constant ρ and to shrink due to mass loss, neglecting for now any pressure driven explosion or distortion which we address later. The changing mass $M(r)$ and 'size' $a(r)$ are then functions of distance r from the solar centre, taking the nucleus orbit to be near parabolic (cf Section 3.1). We treat mass loss (by insolation or ablation) via the simple approximation that a heating/energy deposition rate of $\mathcal{P}$ erg s^{-1} results in mass loss rate $\dot{M}$ g s^{-1} = $\mathcal{P}/\mathcal{L}$ with the relevant ρ, $\mathcal{L}$ values averages over the icy conglomerate components (Sections 2.2.1 and 2.2.3). For the insolation sublimation case the dominant power required for loss of mass from the nucleus is that for sublimation of the ices which then releases the solid dust particles to escape with the vapor outflow. That is, fairly near the sun at least, the power going into sublimation is larger than that going into further heating offset by cooling (Weissman 1993, Sekanina 2003). (Far from the sun our neglect of cooling etc will tend to overestimate the mass loss rate. In any case they should be included in

examining the detailed behavior of the ablated material such as fragmentation and radiation signatures of different ion species - see detailed discussion by Sekanina 2003). For the atmospheric ablation case, heating is intense and vaporizes all components, including the most non-volatile ones. However, as we saw in Section 2.2.3, the overall $\mathcal{L}$ is still comparable to that of the ices. We also recognize that our simple approach applies to comets that are 'active' and thus have nuclei with only a thin covering of insulating dust. However, approach to the sun will thin the dust crust of any comet so our assumption of a porous ice-dominated nucleus is reasonable - Hughes (2000). Even dormant cometary nuclei, which have relatively thicker dust crusts when they are in the terrestrial planetary region of the Solar System, will suffer strong insolation sublimation then collisional ablation as they approach the sun and so speedily re-activate, bearing in mind that even for iron $\mathcal{L}$ is only four times that of ice. We further assume that all mass lost clears the nucleus quickly enough for incident energy fluxes to act directly only on the nucleus - i.e. that the coma and tail produced by the mass loss do not obstruct the processes driving mass loss from the nucleus. To justify this, we note that latent heat $\mathcal{L}$ is equivalent to a speed $\sim 2\mathcal{L}^{1/2} \sim 2.3 \times 10^5$ cm/s. If vaporized material outflow occurs at this speed then, on the timescale $H/v_o \sim 1$ s relevant to atmospheric ablation, it clears nuclei of $a_o \leq 2.3 \times 10^5$ or $M_o \leq 10^{16}$ g so our assumption is justified except for very large masses which are in any case destroyed by explosion rather than ablation. In the case of insolation sublimation the mass loss timescale is much longer (Section 3.3) so the approximation is very good.

Then, for an incident energy flux $\mathcal{F}$ (erg cm^{-2}s^{-1}), $\mathcal{P} \approx a^2 \mathcal{F}$ and, with $a^2 = (M/\rho)^{2/3}$, and constant ρ and shape, we get

$$\dot{M} = \frac{dM}{dt} = -\frac{a^2 \mathcal{F}}{\mathcal{L}} = -\frac{M^{2/3} \mathcal{F}}{\mathcal{L}\rho^{2/3}} \qquad (11)$$

Note that we consider only mass loss in the hemisphere (cross section $\approx a^2$) containing incident flux $\mathcal{F}$ since rotation times are long compared to the short time scale of mass loss near the sun, in contrast with the situation farther from the sun. Using Equation (5) to express $dt = -dr/v_r$ we can eliminate t from Equation (11) and express it as a differential equation for the fractional mass $m = M(r)/M_o$ remaining as a function of r, viz.

$$\frac{1}{m^{2/3}} \frac{dm}{dr} = \frac{R_\odot^{3/2}}{v_\odot} \frac{1}{M_o^{1/3} \mathcal{L}\rho^{2/3}} \frac{\mathcal{F}(r) r^{1/2}}{(1 - q/r)^{1/2}} \qquad (12)$$

This can be integrated for any specified form of $\mathcal{F}(r)$ with boundary condition $m(r \to \infty) = 1$. We have formulated the problem in terms of r dependence since this allows analytic treatment. Conversion to the time domain can be done numerically via Barker's equation (cf results in Porter 2007, 2008).

4.2. Heating Flux Terms and regimes

– The **absorbed insolation flux** is, for albedo $\ll 1$ (e.g. Sekanina 2003)

$$\mathcal{F}_{rad} \approx f \frac{L_\odot}{4\pi r^2} \approx \frac{L_\odot}{4\pi r^2} \approx 5 \times 10^{10} \left(\frac{R_\odot}{r} \right)^2 \text{ erg cm}^{-2} \text{ s}^{-1} \quad (13)$$

where $f(r)$ is the factor by which the heating rate at r differs from our estimate in Equation (13) where we use the $r \gg R_\odot$ approximation of near radial insolation. As $r \to R_\odot$ there is increasing non-radial insolation from the finite solar disk which increases the heating though, for the specific case of

a sphere, provided $r > R_\odot$ then $1 \leq f \leq 2$. However, our approximation of the cross sectional area of a sphere of diameter a as a^2 instead of $\pi a^2/4$ is too large by the factor $4/\pi$ which, for that shape, offsets somewhat the approximation $f \approx 1$ which we use henceforth. Given the quite uncertain shapes of nuclei, this approximation is adequate for our first rough estimates here, especially given the large uncertainties in other parameters and in aspects of the physics.

– the **atmospheric collisional flux** is important since, although the atmospheric mass density is tiny (10^{-7} g cm^{-3} even at the photosphere) compared to that (≈ 1) of the comet nucleus , the specific kinetic energy of the impacting matter $v^2/2 \approx v_\odot^2/2 = 2 \times 10^{15}$ erg/g is, as we have noted in Section 3.1, huge compared to the latent heat of ablation $2.6 \times 10^{10} \tilde{\mathcal{L}}$ erg/g and, in the chromosphere, the ablation flux very large compared with insolation. Impacting solar protons have a collisional mean free path in the comet nucleus material $n \approx 10^{23}$ cm^{-3}) of order 10^{-6} cm (cf. Brown 1972, Emslie 1978). However their mfp in the atmosphere at $n = n_* = 2.5 \times 10^{11}$, where collisions take over from insolation, is $\sim 4 \times 10^5$ cm which is much bigger than all but very massive $\geq 10^{17}$ g nuclei. Furthermore, the nucleus speed is highly supersonic (around Mach 50 in the chromosphere). Thus the bombarding atmospheric protons have neither enough time nor enough collisionality to behave as a fluid - i.e. to flow around the nucleus before impacting it. We therefore treat the problem as one of surface ablation by this particle kinetic flux rather than as a fluid flow with radiaton and heat conduction across a hot shock. (cf. Appendix B). The particle bombardment energy flux is then

$$
\begin{aligned}
\mathcal{F}_{coll}(r) &= \frac{1}{2}\rho_\odot(r)v^3(r) = \frac{1}{2}\mu m_p n(r) v_\odot^3 \left(\frac{R_\odot}{r}\right)^{3/2} \\
&= 2.7 \times 10^{16} \frac{n(r)}{n_\odot}\left(\frac{R_\odot}{r}\right)^{3/2} \quad \text{erg cm}^{-2}\, s^{-1}
\end{aligned}
\tag{14}
$$

(similar to the expression involved in meteor mass loss in the earth's atmosphere - e.g. Kaiser 1961, Chapter 8). Here $n(r)$ is the total (atom + ion) number density (cm^{-3}) of hydrogen, m_p the proton mass and $\mu \approx 1.3$ the mean total mass present (including helium etc) per hydrogen (so that $\rho_\odot = \mu n m_p$) while $n_\odot \approx 10^{17}$ cm^{-3} is the value of n at the photosphere ($r = R_\odot$) which we take as reference point. A detailed model of $n(r)$ over a large range of r was developed by Porter (2007, 2008) and should be used in more precise analysis but, for our first estimates below, we use a simplified exponential atmosphere model which is a fair approximation in the collision dominated region.

– the **ratio of collisional ablation to insolation fluxes** is then

$$
\frac{\mathcal{F}_{coll}(r)}{\mathcal{F}_{rad}(r)} \approx 4 \times 10^5 \left(\frac{r}{R_\odot}\right)^{1/2}\frac{n(r)}{n_\odot} \approx \left(\frac{r}{R_\odot}\right)^{1/2}\frac{n(r)}{n_*}
\tag{15}
$$

where $n_* = n(r_*) \approx 2.5 \times 10^{11}$cm^{-3} is the n value at $r = r_* = 1.01R_\odot$ where $\mathcal{F}_{rad}, \mathcal{F}_{coll}$ are equal. At the photosphere ($n = 10^{17}$ cm^{-3}), $\mathcal{F}_{coll} \approx 10^5 \mathcal{F}_{rad}$ so is equivalent to a black body flux at $T \geq 100,000$ K !

From Equation (15) we see that radiative ablation dominates over collisional only at distances where $n(r) \ll n_* \approx 2.5 \times 10^{11}$ cm^{-3} at which the two are equal. This value $n = n_*$ is in the (upper) chromosphere where the density rises very steeply with depth with a fairly constant temperature (of order 10,000 K) and

hence mean exponential density scale height $H \approx 5 \times 10^7$ cm $\approx 7 \times 10^{-4}R_\odot$, viz.

$$
n(r) = n_\odot e^{-(r-R_\odot)/H}
\tag{16}
$$

(with T, H much higher than for the atmosphere of Jupiter). In this approximation, the values $r = r_*, n = n_*$ thus occur at a height z above the photosphere of $z = z_* = r_* - R_\odot \approx H\ln(4 \times 10^5) \approx 6500$ km $\approx 0.01R_\odot$. Since $h = H/R_\odot \approx 7 \times 10^{-4}$, it follows that, over a very small r range (a few scale heights H) the dominant flux driving mass loss changes rapidly from radiative at $z - z_* \gg H$ to collisional at $z - z_* \ll -H$, a range $\ll R_\odot$. At several scale heights above z_* collisions become negligible compared with radiation so use of analytic expression (16) for $n(r)$ at all heights, though not strictly correct in the corona (where the scale height is much larger), results in negligible error in the total flux. Note that, for $n(r)$ given by Equation (16), over the very narrow range of $1.005 < r/R_\odot < 1.015$ around $r = r_*$, $\mathcal{F}_{rad}(r) \propto r^{-2}$ increases by only 1% while $\mathcal{F}_{coll}(r)$ increases by around $\times 10^6$, which amply vindicates our 'regime switch' approach. Note also that, throughout the present paper, for simplicity we use a height-independent mean value for H. In reality H changes with depth (though very slowly compared to n) since the temperature and hydrogen ionization vary. The variation in H is around a factor of 4 over the entire range $r_* \to R_\odot$ (and far less over the much smaller range of r which proves to be important) while $n(r)$ increases by a factor 10^6. Thus, while the variation in H should be taken into account in more detailed modeling, a constant mean value suffices for the present first discussion of collisional ablation.

From the above discussion, the total flux $\mathcal{F}(r)$ is reasonably well approximated by

$$
\begin{aligned}
\mathcal{F}(r) &= \mathcal{F}_{rad}(r) + \mathcal{F}_{coll}(r) \\
&= \frac{L_\odot}{4\pi r^2} + \frac{1}{2}\mu m_p n_\odot v_\odot^3 e^{-(r-R_\odot)/H}\left(\frac{R_\odot}{r}\right)^{3/2}
\end{aligned}
\tag{17}
$$

If we define dimensionless variables $x = r/R_\odot, m(x) = M(r)/M_o, p = q/R_\odot, h = H/R_\odot$, and use Equation (17) for $\mathcal{F}(r)$, differential equation (11) becomes, with (incoming) boundary condition $m(r \to \infty_-) = 1$

$$
\frac{1}{m^{2/3}}\frac{dm}{dx} = \alpha\left[\frac{1}{x(x-p)^{1/2}} + \beta\frac{e^{-(x-1)/h}}{x^{1/2}(x-p)^{1/2}}\right]
\tag{18}
$$

where the dimensionless parameters α, β are

$$
\alpha = \frac{L_\odot}{4\pi\mathcal{L}\rho^{2/3}v_\odot R_\odot M_o^{1/3}} = \frac{0.27}{\mathcal{M}_{12}^{1/3}} \approx \frac{0.43}{M_{12}^{1/3}}
\tag{19}
$$

where $\mathcal{M}_{12} = \mathcal{M}_o/10^{12}$g, $M_{12} = M_o/10^{12}$g,

$$
\beta = \frac{2\pi\mu m_p R_\odot^2 v_\odot^3 n_\odot}{L_\odot} = 3.8 \times 10^5
\tag{20}
$$

and we define an *effective mass*

$$
\mathcal{M} = \tilde{\mathcal{L}}^3\tilde{\rho}^2 M
\tag{21}
$$

This is the mass scaled relative to the true mass M_o by the factor of $\tilde{\rho}^2\tilde{\mathcal{L}}^3$ and is the mass of water ice which would sublimate at the same rate (g/s) as the actual nucleus mass M_o with its specific values of $\tilde{\rho}, \tilde{\mathcal{L}}$. Note also, for dimensional clarity, that M_{12} and $\mathcal{M}_{12}$ in all equations here are dimensionless, the dimensional scaling unit 10^{12} g being included as a factor in the

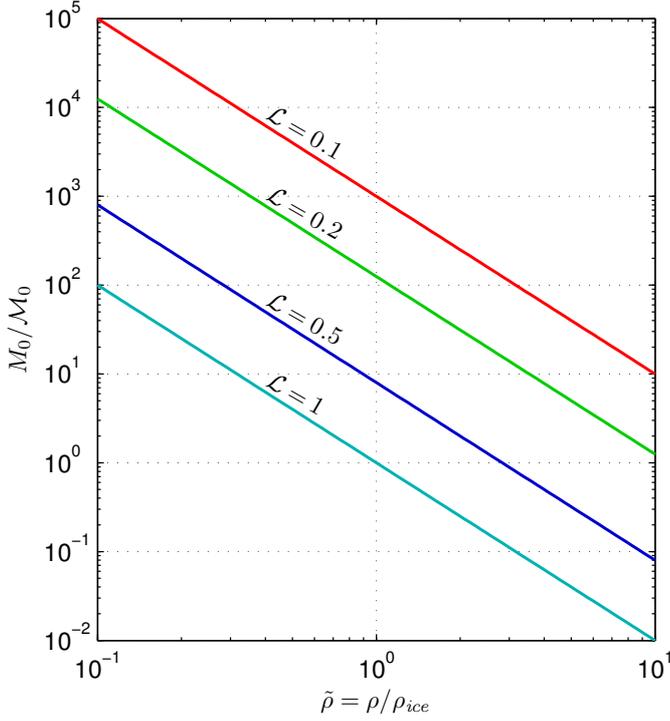**Fig. 1.** Conversion factor $M_o/\mathcal{M}_o$ from ice equivalent mass $\mathcal{M}_o$ to real mass M_o versus $\tilde{\rho}$ for $\tilde{\mathcal{L}} = 0.1, 0.2, 0.5, 1.0$ - Equation (21). For our canonical values $\tilde{\rho} = 0.5, \tilde{\mathcal{L}} = 1$, the true mass $M_o = 4 \times \mathcal{M}_o$ since comet nuclei are less dense than ice so easier to evaporate for given $\mathcal{F}$.

(overall dimensionless) numerical value of α. In Figure 1 we show the dependence of $M_o/\mathcal{M}_o$ on $\tilde{\rho}, \tilde{\mathcal{L}}$. For our canonical values $\tilde{\rho} = 0.5, \tilde{\mathcal{L}} = 1$, the true mass $M_o = 4 \times \mathcal{M}_o$ since comet nuclei are less dense than ice so easier to evaporate for given $\mathcal{F}$.

In cases where the sole processes acting on the nucleus were insolation sublimation and atmospheric ablation (ie hydrodynamic explosion effects were small prior to total vaporisation) the *pure sublimation/ablation solution* $m(x) = M(r)/M_o$ of Equation (18) is, on the inbound trajectory ($\infty_- > x > p$),

$$m(x) = m_-(x) =$$

$$= \left[1 - \frac{\alpha}{3}\left(\int_x^\infty \frac{dx}{x(x-p)^{1/2}} + \beta \int_x^\infty \frac{e^{-(x-1)/h}dx}{x^{1/2}(x-p)^{1/2}}\right)\right]^3$$

$$= \left[1 - \frac{\alpha}{3}\left(\frac{2}{p^{1/2}}\sin^{-1}\left(\frac{p}{x}\right)^{1/2} + \beta \int_x^\infty \frac{e^{-(x-1)/h}dx}{x^{1/2}(x-p)^{1/2}}\right)\right]^3 \quad (22)$$

while on the outbound trajectory ($q < x < \infty_+$) it is (with $\int ..dx = \int_q^\infty ..dx + \int_q^x ..dx$)

$$m(x) = m_+(x) =$$

$$\left[1 - \frac{\alpha}{3} \times \left(\frac{2}{p^{1/2}} \times \left[\pi - \sin^{-1}\left(\frac{p}{x}\right)^{1/2}\right]\right.\right.$$

$$\left.\left. + \beta \times \left(2\int_p^\infty \frac{e^{-(x-1)/h}dx}{x^{1/2}(x-p)^{1/2}} - \int_x^\infty \frac{e^{-(x-1)/h}dx}{x^{1/2}(x-p)^{1/2}}\right)\right)\right]^3 \quad (23)$$

Note that, since $L_\odot, R_\odot, v_\odot, n_\odot, H$ are all known, this pure sublimation/ablation solution $m(x)$ depends solely on the the parameters q and $\mathcal{M}_o$ and we will see below that the combined parameter $\mathcal{M}_o q^{3/2}$ appears frequently in the solution. Conversion from $\mathcal{M}_o$ to M_o of course requires adoption of a value for $\tilde{\rho}^2 \tilde{\mathcal{L}}^3$ - Figure 1.

From the discussion above it is apparent that comets with $q - R_\odot \gtrsim 0.01 R_\odot$ never enter the regime where collisional ablation is important so these can be treated neglecting the collisional terms above. On the other hand comets with $q - R_\odot \lesssim 0.01 R_\odot$, and of large enough $\mathcal{M}_o$ to survive insolation, encounter the collision dominated regime. If, further, they are of large enough $\mathcal{M}_o$ to survive to $r = r_* = 1.01 R_\odot$ with only a *small* mass loss fraction $\Delta m = 1 - m(x_* = r_*/R_\odot) \ll 1$ then their $m(x)$ can be well approximated by including only the collisional ablation terms and neglecting the radiative Δm. These radiative sublimation dominated and atmospheric ablation dominated regimes are treated analytically in Sections 5 and 6.1 while the role of ram pressure driven explosion, vital in the destruction of larger masses at steep impact angle, is discussed in Section 6.2.

5. Insolation Dominated Mass Loss Solutions

($\mathcal{M}_o \lesssim 10^{11}$ or $q - r_* \gg H \approx 0.01 R_\odot$)

5.1. Insolation dominated solution for m(x)

In this case solution (22,23) for $m(x)$ along the incident and outgoing paths become

$$m_-^{rad}(x) = \left[1 - \frac{2\alpha}{3p^{1/2}}\sin^{-1}\left(\frac{p}{x}\right)^{1/2}\right]^3$$

$$\rightarrow \left[1 - \frac{2\alpha}{3x^{1/2}}\right]^3 \text{ as } p \rightarrow 0$$

$$m_+^{rad}(x) = \left[1 - \frac{2\alpha}{3p^{1/2}}\left(\pi - \sin^{-1}\left(\frac{p}{x}\right)^{1/2}\right)\right]^3 \quad (24)$$

which is plotted in Figure 2 in terms of $m(x/p)$ for various values of the parameter $\mathcal{M}_o p^{3/2}$. This Figure can be used for any values of $p, \rho, \mathcal{L}$ because of the scaling and combination of variables used. When modeling nuclei close to perihelion, and comparing models with data, it should be noted that x varies very slowly there and it may be more appropriate to convert the expressions for $m(x)$ etc to the angular variable - i.e. to $m(\theta)$ - or to use the approximation of a horizontal path coordinate.

In the following subsections we discuss features of this solution which are of particular interest.

5.2. Insolation solution properties

5.2.1. Fractional masses remaining and lost by perihelion up to perihelion and after one orbit

By Equation (24) with $x = p = q/R_\odot$, the fractional masses m surviving, and Δm lost by insolation to perihelion are

$$m_q^{rad} = 1 - \Delta m_q^{rad} = \left[1 - \frac{\pi\alpha}{3p^{1/2}}\right]^3$$

$$\approx \left[1 - \frac{0.28}{p^{1/2}M_{12}^{1/3}}\right]^3 \approx \left[1 - \frac{0.7}{p^{1/2}M_{12}^{1/3}}\right]^3 \quad (25)$$

while after one orbit they are, by Equation (24) for $m_+(x \rightarrow \infty)$

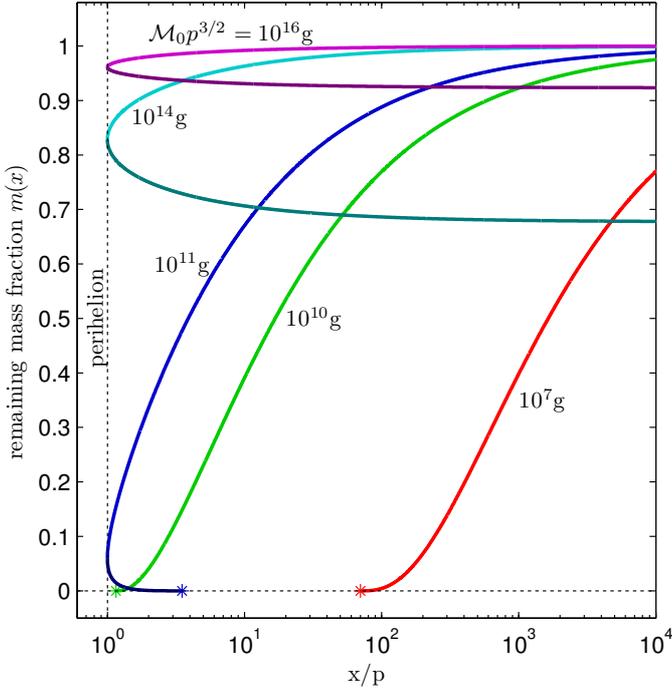$$m_{orbit}^{rad} = 1 - \Delta m_{orbit}^{rad} = \left[1 - \frac{2\pi\alpha}{3p^{1/2}}\right]^3$$

Fig. 2. $m(x)$ versus x/p for various $\mathcal{M}_o p^{3/2}$ showing cases of survival of insolation sublimation through an orbit, and of terminal mass loss before and after perihelion. NOTE that this Figure can be used for any values of $M_o, p, \rho, \mathcal{L}$ because of the scaling and combination of variables used in the Figure.

$$\approx \left[1 - \frac{0.56}{p^{1/2} \mathcal{M}_{12}^{1/3}} \right]^3 \approx \left[1 - \frac{1.4}{p^{1/2} M_{12}^{1/3}} \right]^3 \qquad (26)$$

the last forms being for our canonical $\tilde{\rho}, \tilde{\mathcal{L}}$ values. (These expressions are valid for $p > \pi^2 \alpha^2 / 9, 4\pi^2 \alpha^2 / 9$ respectively). Note that $\Delta m = \Delta M / M_o = \Delta \mathcal{M} / \mathcal{M}_o$, and that the minimum initial mass needed to just survive insolation through one orbit is 8 times that needed to just survive to perihelion (the corresponding minimum a_o values being in the ratio 2:1).

We can rewrite Equation (25) as

$$p^{3/2} \mathcal{M}_{12} = \frac{0.022}{[1 - (1 - \Delta m_q^{rad})^{1/3}]^3} \qquad (27)$$

which lets us evaluate the initial $\mathcal{M}_o \approx 0.25 M_o$ which will lose a fraction Δm by perihelion - see Figure 3 in which the axis variables used allow application to any $p, \tilde{\rho}, \tilde{\mathcal{L}}$.

5.2.2. Minimum initial masses and radii surviving insolation to perihelion and through one orbit

Equations (25, 26) imply the following for the minimum initial masses needed to just survive insolation to perihelion and through one complete orbit.

$$M_{ominq}^{rad}(q) = \frac{\mathcal{M}_{ominq}^{rad}}{\tilde{\mathcal{L}}^3 \tilde{\rho}^2} = \frac{M_{minorbit}^{rad}(q)}{8} = \left[\frac{L_\odot}{12 \mathcal{L} \rho^{2/3} v_\odot R_\odot p^{1/2}} \right]^3$$

$$\approx \frac{2.2 \times 10^{10} \text{g}}{\tilde{\mathcal{L}}^3 \tilde{\rho}^2 p^{3/2}} \approx \frac{8.8 \times 10^{10} \text{g}}{p^{3/2}} \qquad (28)$$

the corresponding minimum initial sizes being

$$a_{ominorbit}^{rad} = 2 a_{ominq}^{rad} \approx \frac{2.7 \times 10^3 \text{ cm}}{\tilde{\mathcal{L}} \tilde{\rho} p^{1/2}} \approx \frac{5.4 \times 10^3 \text{ cm}}{p^{1/2}} \qquad (29)$$
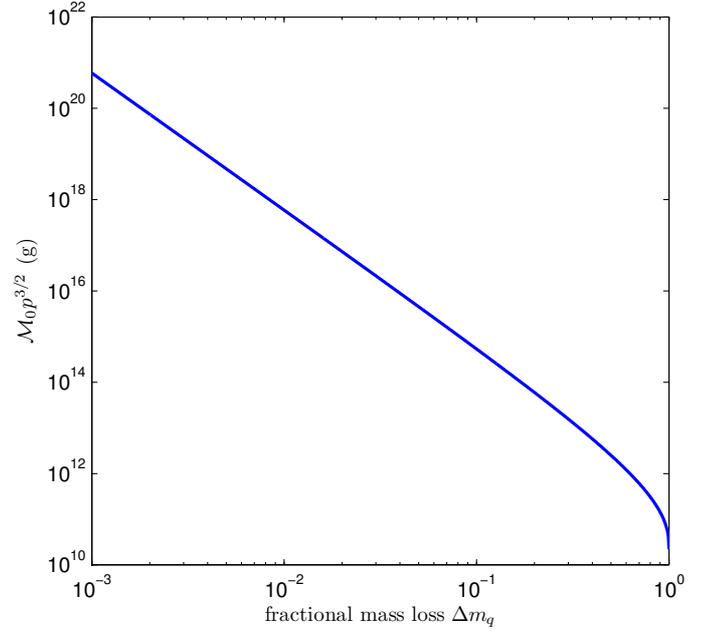

Fig. 3. Value of $\mathcal{M}_o p^{3/2}$ which has undergone fractional insolation sublimation mass loss Δm_q by perihelion - Equation (27). The Figure can be used for any values of $Mo, p, \rho, \mathcal{L}$ because of the scaling and combination of variables used

Consequently (for $\tilde{\rho} = 0.5, \tilde{\mathcal{L}} = 1$) any $M_o \leq 10^{11}$ g with $p \approx 1$ will be totally vaporized by insolation before reaching the ablation zone while the destruction of any $M_o \geq 10^{11}$ g with $p \leq 1.01$ will undergo atmospheric ablation and be totally dominated by it or by explosion, according to the conditions discussed in Sections 3.4 and 6.1-6.2.

The above is a special case, with $x_{end} = p$, of the following

5.2.3. Terminal insolation point

For $M_o < M_{ominq}$ the distance $x_{end}^{rad} R_\odot$ at which insolation mass loss is complete on the inbound trajectory is given by

$$x_{end}^{rad}(q) = \frac{p}{\sin^2 \left(\frac{3 p^{1/2}}{2\alpha} \right)} \approx \frac{p}{\sin^2 (0.56 p^{1/2} \mathcal{M}_{12})}$$

$$\approx \frac{p}{\sin^2 (0.14 p^{1/2} M_{12})} \qquad (30)$$

while, for $M_{ominorbit} > M_o > M_{ominq}$, insolation mass loss is complete on the outbound trajectory at

$$x_{end+}^{rad}(q) = \frac{p}{\sin^2 \left(\pi - \frac{3 p^{1/2}}{2\alpha} \right)} \qquad (31)$$

Note that, in all of the above, the source of the power driving nucleus mass loss by insolation is external - i.e. sunlight - the kinetic energy of the nucleus playing no role. That kinetic energy is carried away in the ablated particles and then dissipated by them in their very short range collisional momentum and energy exchange (deceleration and heating) with the solar atmosphere.

From all of the equations above it is apparent (as anticipated in Section 3.3) that, near the sun, mass loss by sublimation, and the subsequent deposition of kinetic energy and abundance-anomalous matter in the corona occurs over distance scales of order $R_\odot$ or timescales of order $R_\odot / v_\odot$. So even total destruction of the nucleus is more of a slow extended 'fizzle' than an

explosion. This contrasts sharply with the situation of low altitude atmospheric ablation mass loss over a few scale heights $H \approx 10^{-3} R_\odot$ which is directly powered by the huge specific kinetic energy of the nucleus itself. This ultimately produces a very localized abrupt explosion as the nucleus loses its mass and kinetic energy to the lower atmosphere.

5.3. Insolation Sublimation Theory - Comparisons with Numerical Models and with Data

In order to see whether our simple analytic expressions above give reasonable approximations to mass loss, at least for $q \leq$ a few $R_\odot$, we can compare them with those from numerical models incorporating effects we have neglected, such as the early rough numerical thermal modeling by Weissman and Keiffer (1982) and Weissman (1983). Weissman 1983 (his Figure 2) predicts numerically for hypothetical water ice spheres the change Δa resulting from insolation through infall to the photosphere to be $\Delta a \approx 2 \times 10^3$ cm for zero albedo. This can be compared with our expression (29) with $p = 0$ for the value of a_{omin} necessary to survive to the photosphere namely, (with $\tilde{\rho} = 1, \tilde{\mathcal{L}} = 1$ for water ice) $a_{omin} \approx 2.7 \times 10^3$ cm, which is in tolerable agreement with Weissman, given the approximations involved. This gives us confidence in applying our analytic approach to get first rough estimates for the atmospheric ablation regime addressed in Section 6.1, using the smaller value $\tilde{\rho} \approx 0.5$ relevant to the real comet case (Section 2.2.1).

An illustration of how our simple analytic equation can help estimate, or put limits on, comet masses is to consider the very close sun-grazer C/2010 E6 (STEREO) which had an estimated $p \approx 1.020 \pm 0.005$. This was never seen to re-emerge so we can use Equation (29) to put an extreme *upper* limit (orbit survival) on its (effective) mass namely $\mathcal{M}_o < 8 \times 10^{10}$ g or true mass $M_o < 3 \times 10^{11}$ g for $\tilde{\rho} = 0.5, \tilde{\mathcal{L}} = 1$. (This comet's p value was small enough for it to come very close to entering the atmospheric ablation regime). The same can be done for any of the numerous Kreutz Group and other sun-grazers. Though the claim was in fact later dropped, it is interesting to note that if the H-α image claimed by Raftery et al. (2010) had really been comet C/2010 E6 (STEREO) one would know it had survived insolation in to a distance $x \leq 1.05$ and could have put a *lower* limit on its mass using pre-perihelion Equation (24) viz $M_o \geq 4 \times 10^9$ g for our canonical $\tilde{\rho}, \tilde{\mathcal{L}}$ values.

More generally we can see from the Equations above that, if we know q, *any* observed measurement of time integrated mass loss or of local mass loss rate, via our model, estimates of $\mathcal{M}_o, M_o$ can be found. For example, using an observed terminal insolation point x_{end}^{rad} and with p known, Equation (30) could be used to estimate the mass. Even when a nucleus vanishes behind a coronagraph mask at some x and is not seen to re-emerge, an upper limit can be set for $\mathcal{M}_o$ using Equation (31) with $x \leq x_{end+}$.

Finally we note from Equation (25), with $p \approx 1, \tilde{\rho} = 0.5, \tilde{\mathcal{L}} = 1$, that that only nuclei of $q < 1.01 R_\odot$ and $M_o \gtrsim 10^{11}$g can ever reach the depth where atmospheric ablation becomes dominant. Smaller masses are completely sublimated by insolation prior to that point.

6. Ablation and Explosion of Sun-impactors

6.1. Ablation Dominated Solution for Sun Impactors when explosion can be neglected - $M_o(1 - q/r_*)^{3/2} \leq M_{**} \approx 10^{10}$g, $r_* - q \geq H$

For nuclei with $q \leq r_*$ and with original M_o large enough $\geq 10^{11}$ g to survive insolation ablation down to $r < r_*$ the residual mass $M_o' = M_o(1 - \Delta m(x_*))$ has (cf. Section 5.2.1) essentially the same velocity as if it had arrived at r_* without any sublimation. Because of the very rapid large switch from the sublimation to the ablation regime, its subsequent mass loss can thus be treated using only the ablation term in our $m(x)$ expression (22) for a mass M_o' falling from infinity. For simplicity here we will only consider M_o large enough that $\Delta m(x_*) \ll 1$ and simply equate $M_o' = M_o$. Consequently our results for masses in the transition range around 10^{11} g are approximate. In this Section we further restrict ourselves to impactors having small enough M_o and/or shallow enough incidence that atmospheric ablative mass loss is complete before ram pressure driven explosion is significant (explosion of impactors of larger mass and/or impact angle is discussed in Section 6.2). The low and high mass ends of our assumption conditions here encompass the great majority of sungrazers belonging to comet groups such as Kreutz (cf Section 2.3) with $q \leq r_*$. The inbound evolution of $m(x) = M(r)/M_o$ by ablation alone can then be well described by using only the atmospheric ablation terms in Equation (22). (We consider here only the inbound case since the exponentially rising atmospheric density results in total ablation in all cases except for the extremely narrow range $|r_* - q| \leq H$ mentioned above). That is

$$m_-^{coll}(x) = m_{coll}(x) = \left[1 - \frac{\alpha\beta}{3}\int_x^\infty \frac{e^{-(x-1)/h}dx}{x^{1/2}(x-p)^{1/2}}\right]^3 \quad (32)$$

The integral in Equation (32) has in general no standard closed analytic form but, since $h \ll 1$, a good analytic approximation is readily obtained for almost all p. Expression (32) is only physically relevant down to where ablation is complete - viz $\int ..dx \leq 3/\alpha\beta$ - which always occurs close to $x = x_* \approx 1.01$ since $h \ll 1$. Below $x = x_*$ the integrand increases exponentially with depth so is maximal at the x limit of the integral. Consequently, (unlike the exponential numerator) the integrand denominator can be well approximated by setting $x_*(x_* - p))^{1/2} \approx (1 - p/x_*)^{1/2}$ (Rare cases where $|x_* - p| \leq h$ would need a more refined treatment, and inclusion of both ablation and insolation). Solution (32) can then be integrated to give

$$m(x) = m_{coll}(x) \approx \left[1 - \Gamma\frac{e^{-(x-1)/h}}{(1 - p/x_*)^{1/2}}\right]^3 \quad (33)$$

where

$$\Gamma = \frac{\alpha\beta h}{3} = \frac{\mu n_\odot m_p v_\odot^2 H}{6\mathcal{L}\rho^{2/3}M_o^{1/3}} \approx \frac{30}{(\mathcal{M}_o/10^{12})^{1/3}} \quad (34)$$

from which it follows that the nucleus will be totally ablated by the height

$$z_{abl}^{end}(\text{km}) = H \ln \frac{\Gamma}{(1 - p/x_*)^{1/2}}$$

$$2000 + 1100 \times \left[\frac{1}{2}\log_{10}(1 - p/x_*) - \frac{1}{3}\log_{10} M_{12}\right] \quad (35)$$
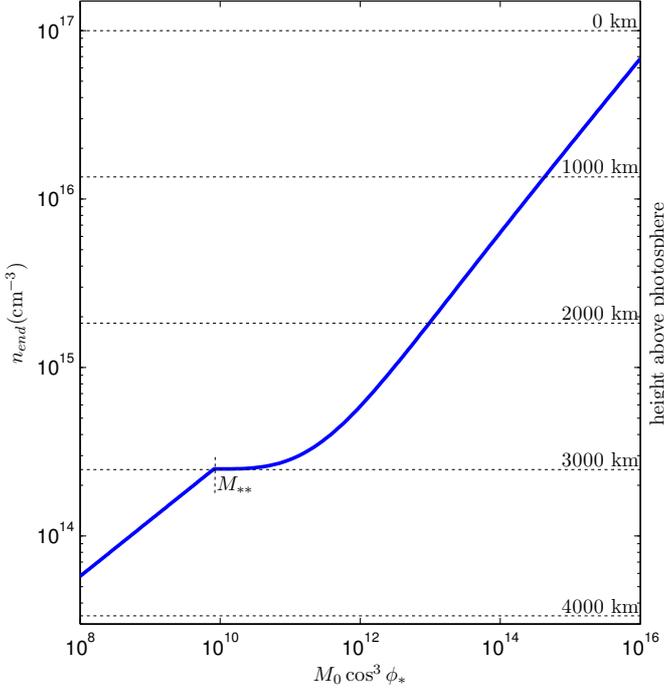
Fig. 4. Estimate of the heights z_{end} and densities n_{end} at which nuclei are essentially destroyed as a function of $M_o \cos^3 \phi_* = M_o (1 - p/x_*)^{3/2}$. To the left of the point labeled M_{**} atmospheric ablation totally vaporizes the nucleus over a few scale heights before ram pressure exceeds the strength of nucleus material. To the right the atmospheric ram pressure drives lateral expansion and explosive disintegration of the nucleus, enhancing both its ablation and deceleration rates, and destroying it in less than a scale height. The 'knee' at M_{abl}^{max} in reality would be a smooth though rapid transition since ram pressure sets in progressively not as a switch. The Figure show that a very large range of masses are destroyed within a few scale heights in the chromosphere. Even a comet as massive as 10^{17} g entering vertically explodes above the photosphere.

with corresponding atmospheric density

$$n_{abl}^{end}(\text{cm}^{-3}) = N_{abl}^{end}/H = \frac{n_\odot(1 - p/x_*)^{1/2}}{\Gamma}$$

$$\approx 1.25 \times 10^{15}(1 - p/x_*)^{1/2} M_{12}^{1/3} \qquad (36)$$

Equation (35) shows that, even neglecting explosion, all cometary nuclei are vaporized by ablation while traversing a few atmospheric scale heights. Such short paths suggest that the ablation path may be approximated as rectilinear, starting around the point where $n \approx n_*$ at angle $\phi \approx \phi_*$ to the vertical, and of nearly constant speed $v_\odot$. From Equations (5) we find that

$$\cos \phi_* = v_r(r_*)/v(r_*) = (1 - p/x_*)^{1/2} \qquad (37)$$

If one re-derives and solves the equation for dm/dx for a rectilinear path one arrives at exactly the same expressions as found in Equations (35, 36) given the relation (37) of ϕ_* to p/x_* so our algebraic approximation there is equivalent to the geometric one of a rectilinear path.

From Equation (9) it then follows that ram pressure driven explosion is small throughout the total ablation phase ($n_{abl}^{end} \leq n_{**} = 2.5 \times 10^{14}$) for masses smaller than

$$M_o \leq M_{abl}^{max}(\phi) = \left[\frac{P_c H}{\tilde{\mathcal{L}} \tilde{\rho}^{2/3}} \right]^3 (1 - p/x_*)^{-3/2} = M_{**} \sec^3 \phi_* =$$

$$\approx \frac{10^{10}}{(1 - p/x_*)^{3/2}} \approx 10^{10} \sec^3 \phi_* \text{ g} \qquad (38)$$

where we have used $P_c H \approx 5 \times 10^{13}$ and $\tilde{\mathcal{L}} = 1, \tilde{\rho} = 0.5$. Here M_{**} is the maximum vertical entry mass which is totally ablated by depth $n = n_{**}$ where ram pressure becomes important. Note that these values of $n_{abl}^{end}, M_{abl}^{max}$ differ by factors of a few from those obtained in Section 3.4.2 due to the more accurate treatment of ablation in Section 6.1 than those estimates. Since $x_* = 1.01$, for the range $1.0099 < p < 1$, the final $\sec^3 \phi_*$ factor is in the range $10^3 - 10^6$ and the mass above which explosion becomes dominant for such grazing impactors is in the range $3 \times 10^{13-16}$ g. This solar limit is much larger than for the conditions of the Shoemaker-Levy 9 Jupiter impacts (with fragment masses estimated to be around 10^{15} g) because of Jupiter's smaller H and the much steeper angle of those impacts (~ 45 deg) which result in a much larger density n and hence ram pressure at a specified $\mathcal{N}$ (which determines ablation) (Section 3.4.2). We conclude that, for grazing solar impacts, our ablation-dominated treatment above is appropriate for up to quite high masses - far larger than that of the vast majority of group comets which have very shallow incidence. However, for the largest masses and for steeper impacts, ram pressure driven explosion of the nucleus becomes crucial. We consider these next, noting that the nucleus hydrodynamic time scale a_o/c_s compared with $H/v_\odot$ implies that these effects will involve total detonation for $a_o \leq 2$ km (around 4×10^{15} g) while in larger nuclei they will initially take the form of front end 'pancaking'.

6.2. Explosion/ablation behavior for nuclei of high $M_o \cos^{3/2} \phi_*$

For nuclei of $M_o > M_{abl}^{max} = M_{**} \sec^3 \phi_*$, i.e. large enough to reach the depth where $P_{ram} \geq P_c$, mass loss from, and destruction of, the nucleus becomes dominated by explosive hydrodynamic expansion. This occurs due to the action of the exponentially growing ram pressure, compounded by breakup of the nucleus and flow through hydrodynamic instabilities as discussed in detail for planetary impacts by Chyba et al (1993), Field and Ferrara (1994), MacLow and Zahnle (1994), Zahnle and MacLow (1994) and Carlson et al (1997). Modeling this intense localised explosion and the subsequent fireball expansion in the solar case is far beyond the scope of the present exploratory paper and should be addressed using modified versions of the numerical simulations conducted for planetary cases. Here we simply describe roughly the initial phases of this explosion process for the solar case to get some indication of what might be seen when a high mass/steep entry solar impact is eventually observed.

If one treats the initial expansion of the nucleus under the effect of the growing ram pressure as a constant density longitudinal shortening but lateral expansion into the low pressure atmosphere one finds (Chyba et al 1993, MacLow and Zhanle 1994 and Field and Ferrara 1994) an approximate expression for how the nucleus radius a initially increases with depth in an exponential atmosphere. This is (e.g. MacLow and Zhanle Equation (2)) for unit drag coefficient (in our notation, and in terms of N)

$$a(N) = H \sec \phi_* \left[\frac{2\mu m_p N}{H\rho} \right]^{1/2} = H \sec \phi_* \left[\frac{2\mu m_p n_\odot e^{-z/H}}{\rho} \right]^{1/2} \qquad (39)$$

with $a(z)$ essentially doubling for every $\Delta z \approx 1.4H$ The resulting growth in area a^2 enhances both the ablation rate and the deceleration, though the latter continues to have a longer time scale since $\mathcal{L} \ll v_\odot^2/2$. In addition (e.g. Field and Ferrara 1994) as time progresses hydrodynamic instabilities rapidly break up the expansion and enhance the dissipation so that the nucleus

essentially explodes, within a very few scale heights, into a hot cloud of plasma and debris (mingled with the intensely heated atmosphere) the deceleration of which is much greater than that of the nucleus. It is of interest to estimate the revised ablation depth arising from the enhanced area given from Equation (39). Integrating the ablating power along the nucleus path s (assuming for now that $v = v_\odot$ - see below) gives the requirement

$$M_o \mathcal{L} = \int_N a^2(N) \mu m_p (v^2/2) dN = (\mu m_p v)^2 \frac{H(N_{abl}^{exp})^2}{2\rho} \sec^3 \phi_* \quad (40)$$

implying

$$N_{abl}^{exp}(\text{cm}^{-2}) = \left[\frac{2 M_o \rho \mathcal{L} \cos^3 \phi_*}{(\mu m_p v_\odot)^2 H} \right]^{1/2}$$

$$\approx 2 \times 10^{23} M_{12}^{1/2} \cos^{3/2} \phi_* (\tilde{\rho} \tilde{\mathcal{L}})^{1/2} \quad (41)$$

Comparing this with result (36) for the total ablation depth in the absence of explosion we find

$$\frac{N_{abl}^{exp}}{N_{abl}} = \frac{3 \cos^{1/2} \phi_* M_{12}^{1/6}}{\tilde{\mathcal{L}}^{1/2} \tilde{\rho}^{1/6}} \quad (42)$$

which is very insensitive to the parameters. If we evaluate it at $M_o = M_{abl}^{max}$ (Equation(10)), where the transition from ablation dominated to exlosion occurs, the value is $\approx 1/(\tilde{\rho}^{1/2} \tilde{\mathcal{L}}^{1/6})$ which is of order unity. So we can roughly split the behaviour into pure ablation and explosion/ablation regimes according to whether $M_o \cos \phi_*^{3/2}$ is $\leq$ or $\geq$ M_{**}. For the pure ablation case, we assume that the ablated ions and small particles in the wake stop very abruptly in collisions with the atmospheric plasma, heating both explosively by conversion of the kinetic energy of the lost nuclear matter. The ablation end depth is then the end point of the nucleus itself.

Nuclei of $M_o \geq M_{abl}^{max}$ enter the regime where $P_{ram} > P_c$ drives explosive lateral expansion. The increasing area results in an accelerated face ablation rate (though it may inhibit escape of the ablated matter) but, more importantly, results in soaring deceleration of the nucleus itself. In this case we will take the nucleus end/destruction depth to be that over which its speed $v(z)$ approaches zero. The equation of motion for speed v is

$$M \frac{d \ln v}{dz} = \mu m_p n(z) a^2(z) \sec \phi_* \quad (43)$$

For the case of explosion, neglecting ablation, with $a(z)$ given by Equation (39) the solution is

$$\frac{v(z)}{v_o} = \exp \left[-\frac{2H}{a_o} \left(\frac{\Sigma(z)}{\Sigma_o} \right)^2 \sec^3 \phi_* \right] \quad (44)$$

so that the Σ scale over which exponentially decaying deceleration occurs is

$$\Sigma_{dec}^{exp} = \left[\left(\frac{a_o}{2H} \right)^{1/2} \cos^{3/2} \phi_* \right] \Sigma_o = \left[\frac{M_o^{1/3} \cos^3 \phi_*}{2\rho^{1/3}H} \right]^{1/2} \Sigma_o$$

$$= 10^{-2} M_{12}^{1/6} \cos^{3/2} \phi_* \Sigma_o \quad (45)$$

where $\Sigma_o = M_o/a_o^2 = M_o^{1/3} \rho^{2/3}$ is the surface mass density g/cm^2 of the nucleus and $\Sigma(z) = \mu m_p \int_0^\infty n(z)dz = \mu m_p H n_\odot e^{-z/H}$ that of the atmosphere above z. On the other hand. in the case of no explosion or ablation ($a(z) = a_o$), the solution is $v(z)/v_o = \exp[-\Sigma(z) \sec \phi_* / \Sigma_o]$ with deceleration scale $\Sigma_{dec} =$

$\Sigma_o \cos \phi_*$ as per our rough estimate in Section 3.4.2. Thus explosion, when it sets in, reduces the Σ stopping scale by a factor $10^{-2} M_{12}^{1/6} \cos^{3/2} \phi_*$ which is very small for any relevant M_o. Note also that in BOTH cases the z scale over which $v(z)$ falls by some factor, say X, then X only increases as $ln(ln(z))$ so almost all of the deceleration and explosive destruction occur within roughly one scale height at a height only logarithmically dependent on M_o etc as we show below.

Unless $M_o \gg M_{abl}^{max}$ the relevant 'injection' mass into the explosion regime is not M_o but the reduced mass M_{red} after (mainly) ablation to that point, given by Equation (33) as

$$M_{red}(M_o, p) = M_o \left[1 - \left(\frac{M_{abl}^{max}(p)}{M_o} \right)^{1/3} \right]^3 \quad (46)$$

Then, replacing M_o by M_{red} in Equation (45), gives the deceleration scale in Σ beyond the ablation regime over which deceleration occurs, viz

$$\Sigma_{dec}^{exp}(M_o, p) = \left(\frac{M_o \rho \cos^3 \phi_*}{2H} \right)^{1/2} \left[1 - \left(\frac{M_{abl}^{max}(p)}{M_o} \right)^{1/3} \right]^{3/2} \quad (47)$$

The atmospheric surface mass density in the ablation regime down to where explosion sets in is, for solar parameters, $\Sigma_{**} = H n_{**} \approx 1.25 \times 10^{22}$ cm^{-2} so the total depth Σ_{exl}^{end} at which masses $M_o \geq M_{abl}^{max}$ undergo explosive destruction is $\Sigma_{exp}^{end} = \Sigma_{dec}^{exp} + \Sigma_{**}$ viz.

$$\Sigma_{exp}^{end} = \Sigma_{**} + \left(\frac{M_o \rho \cos^3 \phi_*}{2H} \right)^{1/2} \left[1 - \left(\frac{M_{abl}^{max}(p)}{M_o} \right)^{1/3} \right]^{3/2} \quad (48)$$

with the corresponding space number density

$$n_{exp}^{end} = n_{**} + \left(\frac{M_o \rho \cos^3 \phi_*}{2H^3 \mu^2 m_p^2} \right)^{1/2} \left[1 - \left(\frac{M_{abl}^{max}(p)}{M_o} \right)^{1/3} \right]^{3/2} =$$

$$2.5 \times 10^{14} \left[1 + 2.8 M_{12}^{1/2} \cos^{3/2} \phi_* \left[1 - \left(\frac{0.01}{M_{12} \cos^3 \phi_*} \right)^{1/3} \right]^{3/2} \right] \quad (49)$$

and height

$$z_{exp}^{end}(\text{km}) = -H \ln \left(\frac{n_{exp}^{end}}{n_\odot} \right) \approx$$

$$3000 - 500 \log_{10} \left[1 + 2.8 M_{12}^{1/2} \cos^{3/2} \phi_* \left[1 - \left(\frac{0.01}{M_{12} \cos^3 \phi_*} \right)^{1/3} \right]^{3/2} \right] \quad (50)$$

Combining the results of Equations (36, 49) and (35, 50) for the ablation and explosion regimes, we show in Fig. 4 the destruction end height and density as a function of $M_o \cos \phi_*$ for a wide range of masses. Note the very small height range for a large mass range.

As a check on our estimates here we can apply Equation (48) to the explosion dominated (large $M_o \cos^3 \phi_*$) case of Shoemaker-Levy-9 impacts with Jupiter and compare it with the results from the various numerical hydrodynamic simulations. For $M_o = 10^{15}$g, $H = 50$km, $\phi_* \approx 45$ deg our estimate of $\Sigma_{exp}^{end} \approx 3000$ g/cm^2 which, for Jovian gravity g_J, implies an atmospheric pressure $\Sigma_{exp}^{end} g_J \approx 10^7$ dyne/cm^2 = 10 bar which is nicely within the quite wide range ($\sim 1 - 100$ bar) of the numerical simulation results depending on how processes like instabilities are treated (see MacLow and Zahnle 1994 and references therein).

6.3. Energy deposition profiles of Sun-impacting comets

To calculate observable diagnostic signatures of the destruction of comets near the sun requires modeling the primary energy deposition profile then calculating the thermal, hydrodynamic, and radiative response of the solar atmosphere - the evolution of the fireball which follows the primary airburst. For the impact case, doing this numerically along somewhat similar lines to planetary impact work by e.g. Carlson et al. (1995, 1997) and other work cited in Sections 3.4.1 and 6.2 is beyond the scope of the present paper and here we simply take a first step by estimating the height distribution of the nucleus kinetic energy deposition for the ablation dominated case, touching briefly on the explosion domain.

In the case of impacts, as we saw in Section 3.3-3.4 the length and timescales of nucleus mass and kinetic energy loss by ablation and explosion are much shorter than for the insolation sublimation case. The destruction properties of the pure ablation case ($M_o(1 - p/x_*)^{3/2} \leq 10^{10}$ g), relevant to the great majority of moderate mass shallow entry sun-grazers, are also rather distinct from the explosion of high mass/steep entry nuclei. In the former (and in the early stages of the latter) nucleus mass and kinetic energy are steadily deposited in the atmosphere by the ablated atoms ions and particles over just a few scale heights. This results in intense heating and explosion of both the ablated wake and of the surrounding atmosphere, creating an air burst and then an expanding rising fireball. In the explosive destruction regime the deposition of mass by explosion and ablation is even more localized and intense as estimated in Section 6.2 but the details will have to be predicted numerically as in e.g. the Jupiter impacts. The ablation case, however, is more amenable to approximate analytic treatment.

The height distribution $d\mathcal{E}/dr$ (erg/cm) of kinetic energy deposited along the ablation path can be approximated by

$$\left[\frac{d\mathcal{E}}{dr}\right]_{abl} \approx \frac{1}{2}v^2(r)M_o\frac{dm}{dr} = \frac{M_o v_\odot^2}{2R_\odot x}\frac{dm}{dx} \approx \frac{M_o v_\odot^2}{2R_\odot}\frac{dm}{dx} \tag{51}$$

since x is very close to unity and v very close to $v_\odot$ over the few scale heights involved.

Using Equation (33) to find dm/dx gives

$$\left[\frac{d\mathcal{E}}{dr}\right]_{abl} \approx \frac{\mathcal{E}_o}{H}\eta\left[1 - \frac{\eta}{\eta_{end}}\right]^2 \tag{52}$$

where the variable $\eta = e^{-(x-1)/h} = n(r)/n_\odot$ measures depth in terms of atmospheric density and $\eta_{end} = (1 - p/x_*)^{1/2}/\Gamma$ is the value $n_{abl}^{end}/n_\odot = e^{-(x_{abl}^{end}-1)/h}$ where ablation is complete (cf Equation (36)). $\mathcal{E}_o$ here is defined by

$$\mathcal{E}_o = \frac{3M_o\Gamma v_\odot^2}{2(1 - p/x_*)^{1/2}} = \frac{10^{28}(M_o/10^{12})^{2/3}}{(1 - p/x_*)^{1/2}\tilde{\mathcal{L}}\tilde{\rho}^{2/3}} \text{ erg} \tag{53}$$

Clearly $d\mathcal{E}/dr$ is very sharply peaked in height z ($\Delta z \approx H$) with a maximum at relative density

$$\eta = \eta_{max} = n_{max}/n_\odot = \eta_{abl}/3 = \frac{(1 - p/x_*)^{1/2}}{3\Gamma} \tag{54}$$

or

$$n_{max}(\text{cm}^{-3}) \approx 2 \times 10^{14}(1 - p/x_*)^{1/2}(M_o/10^{12})^{1/3} \tag{55}$$

the maximum value being

$$\left(\frac{d\mathcal{E}}{dr}\right)_{max} = \frac{4\mathcal{E}_o\eta_{abl}}{27H} = \frac{2M_o v_\odot^2}{9H(1 - p/x_*)^{1/2}}$$

$$\approx 2 \times 10^{19}(M_o/10^{12})\sec\phi_* \text{ erg/cm} \tag{56}$$

In the rare cases of high mass steep entry we have seen in Section 6.2 that the onset of explosion causes rapid deceleration and disintegration of the nucleus. This will result in even higher volumetric heating rates than in the case of pure ablation, though numerical simulations are needed to quantify this. Such atmospheric power input is of similar order to that released in solar magnetic flares (10^{27-30} erg/sec over loop lengths $\sim 10^9$ cm) though it is deposited much more locally and impulsively.

7. Discussion and Conclusions

7.1. Summary of Nucleus Destruction Regimes

We have shown there to be three regimes of nucleus behavior, depending on the values of M_o, q for given values of $\tilde{\rho}, \tilde{\mathcal{L}}$ for which we adopt here $\tilde{\rho} = 0.5, \tilde{\mathcal{L}} = 1$, namely

– (Section 5.2.2, Equation (28))
Nuclei of $p \geq x_*, M_o \leq M_1(p)$ given by

$$M_1(p) = M_{ominq}^{rad} = \frac{M_*}{p^{3/2}} \approx \frac{10^{11}}{p^{3/2}} \text{ g} \tag{57}$$

are completely sublimated by insolation before they reach perihelion, (or r_*) while those of $M_o \geq M_1(x_*)$ and $p \leq x_* = 1.01$ ($n = n_* = 2.5 \times 10^{11}$ cm^{-3}) enter the atmospheric ablation regime where collisions overwhelm insolation.

– (Sections 3.4.2, 6.1) Since $n = n_{**} = 2.5 \times 10^{14}$ at x_{**}, where atmospheric ram pressure starts to exceed nucleus material strength, nuclei with $x_{**} < p < x_*$ and $M_1(p) < M_o < M_2(p)$ (i.e. of sufficiently low mass or shallow entry angle) lose all their mass to ablation before ram pressure driven explosion is significant, with

$$M_2(p) = M_{abl}^{max}(p) = M_{**}(1-p/x*)^{-3/2} \approx 10^{10}(1-p/x*)^{-3/2}\text{g} \tag{58}$$

– (Section 6.2) Nuclei with $M_o > M_2(p)$ (ie of sufficiently high mass or steep entry) undergo ram pressure driven explosion with greatly enhanced ablation and deceleration.

These findings are summarized in Figure 5 as domains in the plane of $(p/x_*, M_o)$.

7.2. Visibility of Sun-grazer destruction by insolation

It was shown in Section 3.3 that destruction by insolation of low mass nuclei even very near the sun occurs over scales $\sim R_\odot$ in space and ~ 1 hr in time, making them hard to observe against solar atmospheric emission and scattering. However, the abrupt collisional stopping of sublimated material in the wake can raise its initial temperature to around 10^7 K which may make it visible in the XUV if it does not cool too quickly by radiation, conduction or expansion and if its emission measure $\int_V n^2 dV$ is high enough. A 10^{11} g mass totally sublimated over a $1R_\odot$ path into a conical wake of half angle say 10^{-2} radians would have an emission measure only of order 10^{40} cm^{-3} and a mean density of just $\sim 10^7$ cm^{-3} in a solar plasma environment of $n \sim 10^{9-10}$ (both values reduced for a larger cone angle). The final destruction event would therefore be hard to detect in scattered light or line emission despite its highly non-solar element abundances though the numbers should be checked against the capabilities of the best instruments available such as those on the Solar Dynamics Observatory.
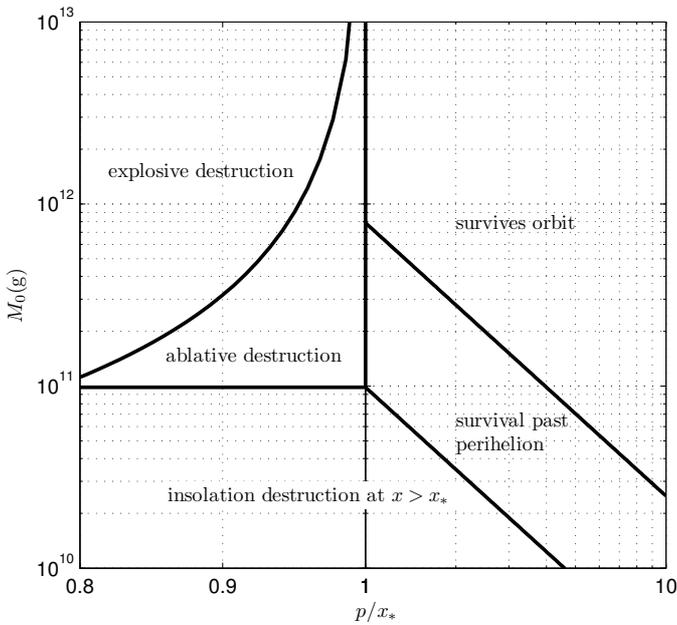
Fig. 5. Domains of destruction of comet nuclei in the plane $(M_o, p/x_* = \sin\phi_*)$ for entry angle $\phi_* = \arcsin(p/x_*)$ to the vertical at $r = r_*$. NOTE the change from linear to log scale on the p/x_* axis across the point $p/x_* = 1$ so as to display the very rapid variation in the range $p/x_* \leq 1$.

7.3. Signatures of Sun-impactor Destruction

7.3.1. Mass, Energy and Temperature of the Fireball

The kinetic energy initially released in the lower solar atmosphere by sun impacting cometary nuclei with $M_o = 10^{11} - 10^{19}$ g is $5 \times (10^{26} - 10^{34})$ erg, similar to the range of the magnetic energy release from 'nano'-flares to 'super'-flares. If 50% of $\mathcal{E}_{kin}$ went into heating the comet material the temperature attainable would be $T > m_p v_\odot^2/4k \approx 10^7 K$ where k is Boltzmann's constant. (Similar T is obtained if we use a fluid shock argument similar to that for collision shocks in stellar winds flows - e.g. Lamers and Cassinelli 1999). This is of order the solar escape temperature since it is generated by infall from ∞. It is comparable with the temperatures of Soft X-ray magnetic flare plasmas which can explode to ∞. In terms of energy conversion, infall heating of cometary matter thus resembles time reversal of thermal ejection of magnetic flare matter.

Flare masses ejected are of the order of 10^{12-16} g, also comparable with those of some impacting cometary nuclei. Thus a comet impact in the dense chromosphere should produce phenomena somewhat resembling a solar (magnetic) flare, though the initial comet volume is much smaller, its density much higher, and the heating rise time faster (seconds). Because of the initially small size scale and high density and pressure we might expect rapid initial cooling (seconds) by radiation, expansion and conduction, followed by a radiative/conductive decay phase more like that of solar flares ($\approx 10^3$ s) as the fireball expands outward and upward, sweeping solar plasma with it (cf. the Carlson et al. 1997 study of the Jupiter impact fireball).

7.3.2. Cometary Flare Size, Emission Measure and Optical Depth

If it is optically thin, the radiative output of a hot plasma of volume V depends on its temperature and its emission measure $EM = \int_V n^2 dV \approx a^3(M_o/\mu_c m_p)^2 \approx 10^{48}(M_o/10^{12})^2/(a/10^8)^3/\mu_c$ cm^{-3} for a nucleus of mass M_o when it has expanded to size a. (Here μ_c is the mean comet mass per particle in units of m_p). Explosion of a nucleus occurs over a few scale heights $\approx 10^7$ cm vertically, traversed in seconds at speed $v_\odot$ (Section 6). If the lateral expansion speed of the hot wake were of order $v_\odot$ then the lateral dimension of the explosion would also be a few H. Its optical depth for a process with absorption cross-section σ would then be $\tau \approx \sigma M_o/m_p a^2 = (M_o/10^{12})(\sigma/10^{-20})/\mu_c/(a/10^8)^2$. Thus when a nucleus of, for example, $M_o = 10^{12}$ g ($a_o \sim 10^4$ cm) becomes optically thin ($a = 10^6$ cm) it has, for $\sigma = 10^{-20}$ cm^2, an $EM \approx 10^{48}$ cm^{-3} (scaling as M_o^2) similar to a medium sized solar flare and easily detectable at $T \approx 10^7$ K in X-ray lines and free-free radio emission. This EM is only for the cometary material itself, but, depending on the atmospheric density at the explosion height, the EM of the heated atmosphere may also be important. Certainly an atmospheric mass larger than that of the ablated nucleus matter is involved in decelerating it. A scale height H is around 1 arcsec so we may expect to see initially a source of a few arcsec expanding at about 1 arcsec per sec at chromospheric altitudes and atmospheric density $\simeq 10^{13-16}$ cm^{-3} depending on M_o as per Figure 4. The XUV line spectra should exhibit highly non-solar abundances as should any matter ejected into space (cf. Iseli et al 2002). There may also be a variety of nonthermal radio and other signatures arising from plasma phenomena driven by the highly supersonic expansion, such as shock and/or turbulent acceleration of electrons and ions and charge separation currents as the ablated matter decelerates in the atmosphere - cf. review by Pégauriér (2007) of fusion pellet ablation physics.

7.3.3. Impact Polarized Line Radiation

Fast streaming ions and electrons excite line radiation which is linearly polarized - e.g. in flares and in stellar jets (Fletcher and Brown 1992, 1995). Comet impacts may also exhibit this though the particle speeds are lower.

7.3.4. Cometary Sunquakes and other solar disturbances

The phenomenon of flare induced sunquakes - waves in the photosphere - discovered by Kosovichev and Zharkova (1998) and now widely studied (e.g. Kosovichev 2006) should also result from the momentum impulse delivered by a cometary impact. All such impacts, however small the comet mass, involve a huge kinetic energy density $\rho v_\odot^2/2 \approx 10^{15}$ erg/cm^3. This is $\sim 10^{10}$ times the thermal energy density of the photosphere or the magnetic energy density in a sunspot, being the energy density of a 40 MegaG magnetic field! Even when the kinetic energy is converted by ablation and ram pressure to heat and kinetic energy of explosion, it is initially spread over only a few scale heights. Hence the explosion energy density of a comet like a Shoemaker-Levy 9 (10^{15} g) is about 10^6 erg/cm^3 or that of a 5 kiloG field and still more than the thermal energy density of the photosphere. Thus, while the total energy of most impacting sun-grazers is small compared to that of large flares and CMEs their energy density is so high that local disruption of magnetic fields and triggering of larger scale events seems likely.

7.4. Conclusions

Our simple analytic treatment of comet nucleus insolation sublimation gives results for mass loss in reasonable agreement with

previous analyses despite our neglect of various effects they included. We have proved that nuclei reaching $p = q/R_\odot \lesssim r_*/R_\odot \approx 1.01$ undergo intense bombardment by solar atmospheric ions (energy 2 keV per nucleon) the rate increasing exponentially with depth on a scale of around 500 km. It follows that, above depth r_* where $n = n_* = 2.5 \times 10^{11}$, evaporative destruction is essentially by insolation only while the behavior of any nucleus surviving insolation sublimation to below this height is dominated by atmospheric collisional effects - ablation and ram pressure driven explosion. This creates an exploding air burst followed by a fireball spreading and rising through the atmosphere similarly to the Shoemaker Levy 9 impacts on Jupiter (e.g. Carlson et al. 1997).

Because of the exponential distribution of atmospheric density and the small atmospheric scale height H (compared to $R_\odot$) the terminal heights of these cometary flares is only logarithmically sensitive to the incoming cometary mass (and to the density and latent heat of the nucleus). It ranges from the upper chromosphere for small to moderate comet masses with typically shallow entry angles to near the photosphere even for very massive steep entry comets. Only comets of large enough mass M_o and steep enough entry angle at the ablation onset depth will reach the point where atmospheric ram pressure drives them to explode.

The ablated matter (atoms and small particles) decelerates very quickly in collisions with the atmosphere, depositing its kinetic energy and momentum over a few scale heights in a few seconds, heating the debris and local solar plasma to X-ray emitting temperatures similar to solar flares and with comparable plasma masses and emission measures. Observing such very small (arcsec) very impulsive (secs) but very luminous 'cometary flares' poses a fascinating challenge but will enable new diagnostics of cometary element abundances from the highly non-solar emission spectra. In addition the downward momentum impulse should generate cometary sunquakes as observable ripples in the photosphere akin to those found in conventional magnetically-energized solar flares. In the case of impacts by the most massive comets (10^{20} g or so) the cometary flare energy release (2×10^{35} erg) is much larger than that of the largest solar flares ever observed. An impact of this magnitude would have very significant terrestrial effects.

Appendix A: Rocket action of nucleus mass loss

The rocket action on comets of the mass loss processes which form the coma and tail is a well known source of long term deviations of comet orbits from purely gravitational. In the case of close sun-grazers and sun impactors, the near-sun passage is very brief (hours) but the rocket action of mass loss might still be relevant. Such action could for example reduce v if it occurred predominantly on the sun-facing hemisphere. This is expected here because nucleus rotation times are typically (Samarishinha et al. 2004) long ($\simeq 0.5$ days) compared to the time $R_\odot/v_\odot \sim 10^3$ sec for the nucleus to traverse even a solar radius, let alone the much smaller scale height H on which the density of the lower solar atmosphere increases exponentially. However, we show below that, in all cases, the high nucleus density ρ results in a very low sublimation velocity u and rocket pressure ρu^2 which can thus be neglected.

- **Rocket effect of insolation sublimation** For downward hemisphere ablation at rate $\dot{M} = a^2 \mathcal{F}_\odot/\mathcal{L}$ near the photosphere (with $\mathcal{F}_\odot = L_\odot/4\pi R_\odot^2$) the speed of ablating material is $u = \dot{M}/\rho a^2$ and the resulting force per unit area is $P_{rad} \approx \rho u^2 = \mathcal{F}^2/\mathcal{L}^2\rho$. The nucleus kinetic energy per unit area is $\mathcal{E} = \rho a v_\odot^2/2$ so the rocket effect would only decelerate the nucleus over a distance $\mathcal{E}/P_{rad} = a(\rho v_\odot \mathcal{L}/\mathcal{F}_\odot)^2 \approx 10^4 R_\odot$ which means that the effect can be ignored.

- **Rocket Effect of Atmospheric Ram Pressure and of Ablating Mass** The high atmospheric ablation rates $\dot{M}$ of sun-grazers might result in a significant rocket pressure force $\rho u^2/2$ from the very dense nucleus matter ablated even at a low speed u under the bombardment of the much more tenuous solar atmosphere - density $< 10^{-7}\rho$. (The situation is rather like 'chromospheric evaporation' of the dense solar atmosphere in flares under the heating action of tenuous beams of accelerated particles. This creates a large pressure gradient and upflow across the transition region density jump - Brown 1973, Craig and Brown 1984). We now show, however, that the rocket effect is in fact small for relevant M_o.

The incident kinetic energy per unit area of the nucleus is $\Sigma_o v^2/2$ where $v \approx v_\odot$ and $\Sigma_o = M_o/a_o^2$ is its incident mass per unit area. As argued in Section 3.1, the atmospheric mass per unit area at which bombardment will have produced total ablation of the nucleus is $\Sigma_{abl} \approx \Sigma_o \mathcal{L}/2v^2 \approx 10^{-5}\Sigma_o$, while the atmospheric mass per unit area at which the atmospheric bombardment ram pressure would have decelerated the nucleus is $\Sigma_{ram} \approx \Sigma_o$. Consequently ram pressure deceleration of the nucleus remains negligible throughout its total ablation. On the other hand, the reactive pressure (rocket) force due to ablation at speed u is $P_{rkt} = \rho u^2/2 \approx \rho(\dot{M}/\rho a^2)^2/2 \approx (v^2/2\mathcal{L})^2 \rho_\odot^2 v^2/2\rho$ where $\rho_\odot(r)$ is the local solar mass density at r and the corresponding mass per unit area is $\Sigma_\odot(r) = \int_r^\infty \rho_\odot(r)dr$. The value Σ_{rkt} of $\Sigma_\odot$ at which P_{rkt} would have decelerated the nucleus is then such that $\int P_{rkt}(r)dr \approx \Sigma_o v^2/2$, i.e.

$$\int P_{rkt}dr = \frac{v^2}{2}\rho\left(\frac{v^2}{2\mathcal{L}}\right)^2 \int \rho_\odot^2 dr = \left(\frac{v^2}{2\mathcal{L}}\right)^2 \frac{v^2}{4H\rho}\Sigma_\odot^2 \quad\quad (A.1)$$

Consequently

$$\Sigma_{rkt} \approx \frac{2\mathcal{L}}{v^2}(\Sigma_o H\rho)^{1/2} \quad\quad (A.2)$$

and

$$\frac{\Sigma_{abl}}{\Sigma_{rkt}} \approx \left(\frac{\Sigma_o}{2H\rho}\right)^{1/2} \approx \left(\frac{a_o}{2H}\right)^{1/2} \approx 0.01 M_{12}^{1/6} \quad\quad (A.3)$$

which would only approach unity for huge masses.

Appendix B: Factors Possibly Limiting Ablation

In considering atmospheric drag and ablation mass loss we have taken the nucleus effective area to equal its geometrical area, effectively taking the drag coefficient and energy transfer efficiency as unity and taking the atmospheric particles delivering energy flux $\mathcal{F}_{coll}$ as impacting the nucleus directly rather than flowing around it as a fluid. This will tend to overestimate the mass loss and deceleration rates. The solar atmospheric density n is about $10\times$ lower than Jupiter's at the same N and the flow speed v over 10 times higher so the solar collisionality $\sim n/v^3$ more than 10^4 times lower and the particle treatment more realistic. It has been argued in the planetary case (Petrov and Stulov 1975, Chyba et al 1993, Zhanle and MacLow 1994) that ablation in fact occurs due to radiation from a stand off shock. This would immediately reduce $\mathcal{F}$ by a factor of order 2 since the radiation is isotropic. In addition, these authors argue that the temperature T of the shock is limited by the need for the incident flux $\mathcal{F}$ to dissociate and ionize hydrogen. So, as in the protostar formation the Hayashi/Heyney track there is a range of heating rates over which the main effect is to increase the ionization at the expense of T. Hydrogen ionization becomes substantial at $T \sim 10^4$ K attaining which requires $kT/m_p \approx 10^{12}$ erg/g which is $\sim 40 \times \mathcal{L}_{ice}$. They conclude that the effectiveness of ablation declines with depth (increasing density) in a planetary atmosphere relative to the approximation we are using. To the extent that this is true for the sun, our estimates here will tend to overemphasize ablation versus explosion and give too high a value for M_{abl}^{max} and for the depth N at which explosion starts to dominate. However, the situation is the solar case is less extreme for several reasons. First, the ambient solar chromosphere is around 100 times hotter than Jupiter's atmosphere, so requires less heating, and is already substantially ionized except in its deepest layers. Second, solar impacting protons have keV kinetic energies - far higher than H ionization energy (13.6

eV) while Jupiter impacts are around 10 eV so that direct impact ionization is important in the sun but not Jupiter. Thirdly, the ionization-limited temperatures quoted for the planetary cases are $T \sim 30,000$ K corresponding to a black body flux $\sim 4 \times 10^{13}$ erg/s/cm^3. This is is equivalent to the solar atmospheric bombardment flux at a depth where $n \sim 4 \times 10^{13}$ cm^{-3}, quite deep in the atmosphere (compared to $n = n_*$). Shock temperatures of order $T \sim 10,000 - 100,000$ K are what one expects from the simple conversion of bulk flow of speed $v \sim 50$ km/s into heat across a shock, viz $kT \sim m_p v^2$ while for $v \sim 600$ km/s we expect temperatures around 100 times higher as in X-ray emitting shocks in stellar winds which have similarly high speeds (Lamers and Cassinelli 1999). Thus we will take the view that the H-ionization/shock temperature limitation on the effectiveness of ablation is much less important for solar than for planetary impacts, though more detailed work on this should be carried out.

References

Brown, J.C. : 1972 Solar Phys 26, 441.

Brown, J.C. :1973 Solar Phys 31,143.

Carlson, R. W., Weissman, P. R., Segura, M., Hui, J., Smythe, W. D., Johnson, T. V., Baines, K. H., Drossart, P., Encrenaz, Th., & Leader, F. E. : 1995, Geophys. Res. Lett. 22, 12, 1557.

Carlson R.W., Drossant P.,Encrenaz Th., Weissman P.R., Hui J. & Segura M. 1997, Icarus 128,251.

Chat, G. le : 2006, Internal Report, University of Glasgow.

Chen, D. & Zhang,K. 1996 Earth, Moon and Planets 73,23.

Chevalier R.A. & Sarazin C.L. 1994 ApJ 429, 863

Chyba C.F. Thomas, P.J. & Zahnle K.J.: 1993, Nature 361, 40.

Craig, I.J.D. & Brown 1984, Astron. Astrophys.130, L5.

Emslie, A.G. : 1978, Astrophys, J. 224,241.

Field G.B & Ferrara A. 1995, ApJ 438, 957.

Fletcher, L. & Brown J.C. 1992, Astron Astrophys 259, L43.

Fletcher, L. & Brown J.C. 1995, Astron. Astrophys. 294, 260.

Huebner, W.F.: 1967, Zeit, fur Astrophys, 65, 185.

Huebner W.F., Benkhoff J., Capria M.-T., Coradini A.. De Sanctis C, Orosei R & Prialnik D. 2006, ISSI Scientific Report SR-004, *Heat and Gas Diffusion in Comet Nuclei*

Hughes, D.W. : 1984, Mon Not Roy Astr. Soc. 213, 103.

Hughes, D.W. 2000 Monthly Notices, Royal Astron. Soc. 316, 642.

Hughes, D.W. 2001 Monthly Notices, Royal Astron. Soc. 326, 515.

Iseli M. ,Kuppers M., Benz W., Bochsler, P : 2002, Icarus 350.

Kaiser, T.R. : 1962, *Meteor science and engineering* : McGraw-Hill, London.

Kosovichev, A. G. & Zharkova, V. V. :1998, Nature 393, 317.

Kosovichev, A. G.: 2006, Solar Phys. 238, 1.

Lamers, H. & Cassinelli, J.P. : 1999, *Introduction to Stellar Winds*, Cambridge UP ISBN:0521593980.

MacLow, M.-M. & Zhanle K. 1994. ApJ 434, L33.

McKinley, D.W.R. 1961, *Meteor Science and Engineering*. McGraw-Hill, New York.

Marsden, B.G.: 2005, Ann. Rev. Astron. Astrophys. 43,75.

Mendis, D.A. and Wickramasinghe, N.C. 1975 Ap&SS 37, L13.

Moradi, H., Donea, A.-C., Lindsey, C., Besliu-Ionescu, D., Cally, P.S. :2008, Mon Not Roy Astron Soc 374, 1155.

Pégouriéz, B. : 2007, Plasma Phys. Control. Fusion 49, R87.

Petrov, C.I. , & Stulov, V.P. : 1975, Kosmicheskie Issledonvaniya 13, 587.

Porter, L.J. 2007, RSE Cormack Project Report, Glasgow University..

Porter, L.J. 2008, MSci Project Report, Glasgow University.

Raftery, C. L., Martinez-Oliveros, J. C., Saint-Hilaire, P. & Krucker, S., 2010 AAS Meeting #216, #407.23

Revelle, D.O. : 1979, Journal of Atmospheric and Terrestrial Physics 41, 453.

Sekanina, Z: 1982, Astron, Journal 87, 1059.

Sekanina, Z: 2002, Astrophys. J., 566, 577.

Sekanina, Z: 2003, Astrophys. J., 597, 1237.

Samarashinha, N. H., Mueller, B. E. A., Belton, M. J. S. & Jorda, L., in *Comets II*, ed Festou, M. C., Keller, H. U. and Weaver, H. A., University of Arizona Press, 2004, p. 281 - 299.

Weissman, P.R. :1983, Icarus 55, 448.

Weissman, P.R. & Keiffer, H.H. :1982, Icarus, 47, 302.

Weissman,P.R. & Lowry S.C. 2008, MPS 43,1033.

Whipple, F. 1950, AJ 55, 83.

Zhanle, K. & MacLow M.-M. 1994, Icarus 108,1.